it is difficult to characterize the cells. *Ex vivo*–expanded BMSCs may show interindividual differences and may be contaminated by fibroblasts or other cells. To more precisely characterize BMSCs and control the quality of transplants, reliable molecular markers for BMSCs are required.

Using DNA microarrays, we recently identified four genes expressed at higher levels and eight genes expressed at lower levels in BMSCs than in fibroblasts.[27] However, four positive markers may be insufficient for characterization of BMSCs because of large interindividual differences. In fact, many candidate genes obtained in DNA microarray analyses did not show significant differential expression, when numerous BMSC and fibroblast lines were examined by RT-PCR.[27] It was difficult to determine the expression levels of many candidate genes quantitatively and simultaneously by conventional assay. Accordingly, in the present study, we utilized a TaqMan Low Density Array with 96 ready-made primer and probe sets, which can precisely distinguish interindividual differences from cell type–dependent differences among numerous BMSC and fibroblast samples. This allowed us to make a list of BMSC marker genes that were all consistently expressed at high levels in various BMSC lines in quantitative RT-PCR analysis.

Human BMSCs are usually isolated from the ilium, but alveolar/jaw BMSCs (A-BMSCs) may also be useful in cell therapy for jaw bone defects and periodontal diseases, and orthopedists may elect to use femur or tibia BMSCs (F-BMSCs or T-BMSCs, respectively) for their patients. Although we found that A-BMSCs had less chondrogenic and adipogenic potential than iliac BMSCs (I-BMSCs),[11] the differentiation potential of human F-BMSCs or T-BMSCs had not previously been compared with that of I-BMSCs or A-BMSCs. I-BMSCs, A-BMSCs, F-BMSCs, and T-BMSCs may have distinct differentiation potentials with distinct mRNA expression profiles, and these BMSCs may have common and *in vivo* location–dependent markers, which are expressed at higher levels in BMSCs than in fibroblasts. Furthermore, the expression of BMSC markers may be altered by donor age and passage number, and it is essential to understand the effects of interindividual differences, age, and passage number before application of BMSC markers to tissue engineering.

We showed here that the differentiation potentials and the gene expression profiles of human F-BMSCs and T-BMSCs were similar to those of I-BMSCs, but not A-BMSCs, perhaps because iliac and long bones, and the jaw are derived from the mesoderm and the ectoderm, respectively. In addition, we identified many common makers for I-BMSCs, F-BMSCs, T-BMSCs, and A-BMSCs by real-time RT-PCR with low-density array cards. We found that some markers were useful in clinical studies even when affected by interindividual differences, age, and passage number. We selected BMSC markers for optimal assays—considering the effects of *in vivo* location of BMSCs, interindividual differences, age, and passage number and the magnitude of increase in expression levels—to determine a reliable list of BMSC markers. This list may be useful in increasing the efficacy of tissue engineering and cell-based therapy.

MATERIALS AND METHODS

Cell cultures

BMSCs were obtained from various bones according to protocol approved by ethical authorities at Hiroshima University, or purchased from BioWhittaker (Walkersville, MD). For isolation of A-BMSCs, we selected 12 dental patients (age 19, 23, 24, 25, 25, 25, 43, 55, 57, 59, 63, and 63 years) whose bone marrow sites had been opened during jaw reconstitution surgery or other oral surgery for jaw distortion, jaw fracture, implant operation, tumor resection, or cyst resection; marrow aspirates were obtained using routine syringes and needles as described previously.[11] I-BMSC lines were obtained from four healthy donors (age 18, 18, 19, and 24 years), eight patients with vascular diseases (arteriosclerosis obliterans or Buerger's disease) (age 22, 25, 39, 53, 55, 59, 65, and 81 years), one patient with jaw deformation (age 64), and one patient with diabetes (age 61). Iliac bone marrow was aspirated using puncture needles and syringes. F-BMSC lines were obtained from three patients with malum coxae (age 67, 70, and 70 years) and three patients with injured crucial ligaments (age 17, 22, and 37 years) during surgery. We could not detect any correlation between the diseases and marker gene expression levels (data not shown). Marrow aspirates were immediately mixed with Dulbecco's modified Eagle's medium (DMEM) (Sigma, St. Louis, MO) supplemented with 200 units/mL heparin. The cells were centrifuged at 500 *g* for 5 min and resuspended with DMEM without heparin. Bone marrow cells, including erythrocytes, were seeded at a density of 0.1 mL aspirate per 35 mm tissue culture dish (Corning, Nagog Park Acton, MA) and maintained in 2 mL DMEM (Sigma) supplemented with 10% fetal bovine serum (FBS) (Hyclone, Logan, UT), 100 U/mL penicillin G (Sigma), and 100 μg/mL streptomycin (Sigma) (medium A) at 37°C in a 5% carbon dioxide incubator. Three days after seeding, floating cells were removed and the medium was replaced by fresh medium A. Thereafter, attached cells (plastic-adherent marrow cells) were fed with fresh medium A supplemented with 1 ng/mL fibroblast growth factor-2 (FGF-2) (Kaken Pharmaceutical, Tokyo, Japan), which was added every other day. Passages were performed when cells were approaching confluence. The cells were seeded at a density of 5×10^3 cells/cm^2 on 100 mm tissue culture dishes (Corning) and maintained in 10 mL medium A supplemented with 1 ng/mL FGF-2.[9] To avoid any direct effect of FGF-2 on gene expression, FGF-2 was removed from the culture medium of BMSCs or fibroblasts 72 h before isolation of RNA.

Human skin fibroblasts from five healthy donors (age 29, 33, 36, 45, and 47 years) were purchased from Kurabo (Osaka, Japan), and gum fibroblasts were isolated from four healthy donors (age 17, 18, 26, and 73 years), as described previously.[28] Fibroblast cultures at passages 5–10 were used throughout this study.

Differentiation of BMSCs

Osteogenic, chondrogenic, and adipogenic conversions of BMSCs were determined according to procedures reported by Pittenger *et al.*[1] with some modifications in seeding cell density and duration of cultures. For osteogenic differentiation, cells were seeded at 4×10^4 cells/16 mm well (2.3×10^4 cells/cm^2) and maintained for 28 days in DMEM supplemented with 10% FBS, 10 mM glycerophosphate (Tokyo Kasei Kogyo, Tokyo, Japan), 100 nM dexamethasone (Sigma), and 50 μg/mL ascorbic acid-2-phosphate (Sigma) (osteogenic induction medium). For chondrogenic differentiation, cells were seeded at 2.5×10^5 cells/15 mL plastic centrifuge tube and maintained for 28 days in 0.5 mL of serum-free alpha minimum essential medium (α-MEM) (Sigma) supplemented with 1% insulin–transferrin–selenium plus (ITS-plus) (6.25 μg/mL insulin, 6.25 μg/mL transferrin, 6.25 μg/mL selenite, 5.33 μg/mL linolate, and 1.25 mg/mL bovine serum albumin) (BD Biosciences, San Jose, CA), 10 ng/mL transforming growth factor-β3 (R&D Systems, Minneapolis, MN), 100 nM dexamethasone, and 50 μg/mL ascorbic acid-2-phosphate. The cultures were incubated in 0.5 mL of the medium until 3 days after seeding, and thereafter the cultures were fed with 1 mL of the medium every other day. For adipogenic differentiation, cells were seeded at 2×10^5 cells/35 mm well (2.3×10^4 cells/cm^2) and grown to confluence in medium A. Adipogenic differentiation was induced by subjecting confluent monolayers to three rounds of adipogenic treatment. Each round consisted of incubation with DMEM (high glucose) (Sigma) containing 10% FBS, 0.2 mM indomethacin (Wako, Osaka, Japan), 1 μM dexamethasone, 0.5 mM 3-isobutyl-1-methyl-xanthine (Wako), and 10 μg/mL insulin (Wako) (adipogenic induction medium) for 72–96 h, followed by incubation with DMEM (high glucose) containing 10% FBS and 10 μg/mL insulin (maintenance medium) for another 72–96 h. Cultures were maintained for 28 days.

Calcium, glycosaminoglycan, and glycerol 3-phosphate dehydrogenase activity

Calcium levels were determined by the method of Gitelman.[29] Cartilage pellets were digested with 300 μg/mL papain (Wako) in the presence of 2 mM ethylenediaminetetraacetic acid (EDTA), 2 mM N-acetylcysteine, and 50 mM sodium/potassium phosphate buffer (pH 6.5) at 60°C for 1 h, and the glycosaminoglycan (GAG) content was determined using a sulfated GAG assay kit (Biocolor, Newtownabbey, Northern Ireland).[30] Glycerol 3-phosphate dehydrogenase (GPDH) activity was determined using a GPDH activity assay kit (Hokudo, Sapporo, Japan).[31]

Microarray analysis

Total RNA was extracted using TRIZOL reagent (Invitrogen, Carlsbad, CA), when the fifth to eighth passage cultures became confluent. Poly $(A)^+$ RNA was purified using Micro poly (A) purist (Ambion, Austin, TX). DNA microarray analysis was performed with 0.5 μg poly $(A)^+$ RNA from A-BMSC ($n=1$) and I-BMSC ($n=1$) lines and skin ($n=1$) and gum ($n=1$) fibroblast lines using Kurabo Life Array analysis service (Incyte Genomics; Lot# KL01081 and Motorola; CodeLink-UniSet Human I). Incyte Genomics (UniGEM V2.0) uses Incyte DNA clones and two-color method. The expression level was deduced from the ratio of hybridization signal intensity (Cy5/Cy3) using Balance Coefficient and GEMTools 2.5 Software (Incyte Genomics, www.incyte.com). Motorola (CodeLink-UniSet Human I Bioarray) uses high-density oligonucleotide arrays and monocolor method. The hybridization signal on different chips was normalized using the median level and Code Link™ System Software Analysis Version 2.2.2. (www.amershambiosciences.com).

Quantitative RT-PCR

Total RNA was isolated using RNeasy minicolumns and reagents (Qiagen, Hilden, Germany), when the primary to 10th passage cultures became confluent. DNase I (Ambion) treatment was performed to remove genomic DNA from RNA samples according to the manufacturer's protocol. The first-strand cDNA was synthesized from 1 μg of total RNA using the ReverTra Ace-α (Toyobo, Osaka, Japan). Real-time quantitative PCR was performed using ABI Prism 7900 Sequence Detection System Instrument and Software (Applied Biosystems, Foster City, CA) with a TaqMan Low Density Array (Applied Biosystems). The TaqMan Low Density Array was designed for custom assay configuration with selected ready-made probe and primer sets. The mRNA level relative to that of β-actin was calculated. We normalized mRNA levels in various BMSCs against the values obtained with fibroblasts.

Enzyme-linked immunosorbent assay

BMSCs and fibroblasts were seeded in 100 mm tissue culture dishes at a density of 5×10^3 cells/cm^2, and maintained in 10 mL medium A supplemented with 1 ng/mL FGF-2 for 7 days. The cells were preincubated with DMEM/Ham's F-12 containing 10% FBS for 24 h. Thereafter, the cells were incubated with DMEM/Ham's F-12 containing 1% or 10% FBS for 24 h. Vascular endothelial growth factor (VEGF) and pro-matrix metalloproteinase 1 (pro-MMP1) in

the medium containing 1% FBS and leukemia inhibitory factor (LIF) in the medium containing 10% FBS were determined using Quantikine Immunoassays (R&D Systems).

Quantitation of DNA

Quantitation of genomic DNA was determined using PicoGreen fluorescence assays (Invitrogen).

Statistical analysis

Data are represented by mean ± standard error of the mean (SEM). Comparison of the effects of various treatments was performed with Pearson and Student's *t*-tests. Values of p less than 0.05 were considered statistically significant.

RESULTS

Osteogenic, chondrogenic, and adipogenic differentiations of BMSCs isolated from various bones

Osteogenic, chondrogenic, and adipogenic differentiations in F-BMSC, T-BMSC, I-BMSC, and A-BMSC lines were compared after incubation with the appropriate differentiation induction medium for 28 days. Calcium levels of all BMSC lines increased in the osteogenic condition (OS+) compared with those in medium A (OS−) (Fig. 1A). In chondrogenic or adipogenic conditions, I-BMSC, F-BMSC, and T-BMSC lines showed a marked increase in GAG contents or GPDH activities, respectively (Fig. 1B, C). However, A-BMSCs did not show any differentiation into chondrocytes or adipocytes under these culture conditions, as was expected from results of a previous study.[11] The osteogenic, chondrogenic, and adipogenic potentials of F-BMSCs and T-BMSCs were similar to that of I-BMSCs. In Figure 1, the chondrogenic and adipogenic potentials of A-BMSCs were undetectable, but some A-BMSC lines exhibited low levels of the chondrogenic and adipogenic potentials when cultured for an extended period.[11]

Comparison of gene expression levels between BMSCs and fibroblasts

To identify BMSC marker genes, we compared gene expression profiles between A-BMSCs and skin fibroblasts, using DNA microarrays containing probes for 9,026 genes (Exp. 1), and between I-BMSCs and gum fibroblasts, using those containing probes for 9,962 genes (Exp. 2). The DNA microarrays used in Exp. 1 and 2 contained probes for 1,285 common genes. In these studies, 62 and 114 genes showed greater than twofold higher expression in A-BMSCs and I-BMSCs, respectively, than in fibroblasts: two genes were identified in both Exp. 1 and 2. To confirm their enhanced expression in all BMSC lines, we used TaqMan Low Density Array–containing primers and probe sets for 35 and 62 (two overlap) genes, which had been identified in Exp. 1 and 2, respectively. Only 29 of 95 genes showed significantly higher expression levels in A-BMSC and/or I-BMSC lines than in fibroblast lines in the presence of large inter-individual differences (Table 1). In Table 1, we normalized mRNA levels in various BMSCs against the values obtained with fibroblasts.

We categorized these 29 genes into four groups (A-1, A-2, B, and C) (Table 1). Group A-1 genes ($n = 13$) showed significantly ($p < 0.05$) higher expression levels in both A-BMSCs and I-BMSCs than in fibroblasts. Group A-2 genes ($n = 11$) showed significantly ($p < 0.05$) higher expression levels in either A-BMSCs or I-BMSCs than in fibroblasts, and showed at least threefold higher expression levels in other BMSCs than in fibroblasts, although some of these levels were not statistically significant. Groups A-1 and A-2 genes were thus considered to be common markers for BMSCs.

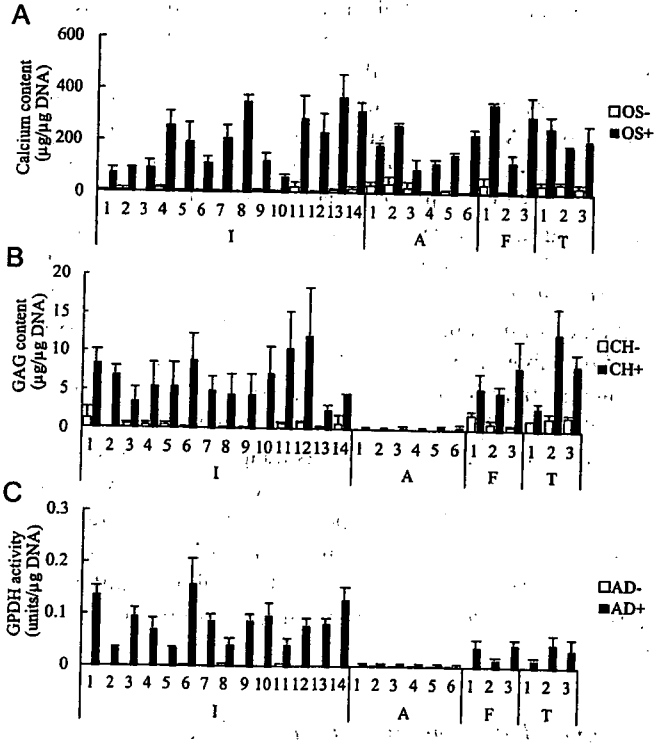

FIG. 1. The differentiation potential of I-BMSCs (I), A-BMSCs (A), F-BMSCs (F), and T-BMSCs (T). (**A**) Cultures of BMSCs obtained at passages 4–6 were maintained in medium A (OS−) or in the osteogenic medium (OS+). The calcium level was determined on day 28. (**B**) Pellet cultures were maintained in medium A (CH−) or in the chondrogenic medium (CH+). The GAG content was determined on day 28. (**C**) Cultures were maintained in medium A (AD−) or in the adipogenic medium (AD+). GPDH activity was determined on day 28. The values are mean ± SEM for three cultures.

TABLE 1. COMMON AND *IN VIVO*-LOCATION DEPENDENT MARKERS FOR BMSC AND RELATIVE MRNA EXPRESSION LEVELS IN I-BMSC, A-BMSC AND FIBROBLASTS

Group	Gene symbol	Gene titles	Relative mRNA levels		
			I-BMSC	A-BMSC	Fibroblasts
A-1	ADD3	adducin 3 (gamma)	3 ± 1*	9 ± 1*	1 ± 1
	BMP4	bone morphogenetic protein 4	58 ± 19*	199 ± 54*	1 ± 1
	CTGF	connective tissue growth factor	15 ± 3*	13 ± 4*	1 ± 0
	IGF1	insulin-like growth factor 1	356 ± 124*	535 ± 138*	1 ± 1
	IGFBP7	insulin-like growth factor binding protein 7	21 ± 7*	22 ± 7*	1 ± 1
	KCTD12	potassium channel tetramerisation domain containing 12	14 ± 3*	15 ± 2*	1 ± 0
	LAMA3	laminin, alpha 3	14 ± 4*	17 ± 3*	1 ± 0
	LIF	leukemia inhibitory factor	41 ± 12*	22 ± 7*	1 ± 1
	MGP	matrix Gla protein	66 ± 25*	60 ± 19*	1 ± 1
	PRG1	proteoglycan 1, secretory granule	181 ± 66*	86 ± 29*	1 ± 0
	SERPINI1#	serine (or cysteine) proteinase inhibitor, clade I (neuroserpin), member 1	28 ± 8*	79 ± 11*	1 ± 1
	TRIB2	tribbles homolog 2	8 ± 2*	10 ± 3*	1 ± 0
	VEGF	vascular endothelial growth factor	4 ± 1*	3 ± 1*	1 ± 0
A-2	ARHGDIB	Rho GDP dissociation inhibitor (GDI) beta	8 ± 3*	6 ± 3	1 ± 1
	CD74#	CD74 antigen	247 ± 87*	14 ± 5	1 ± 1
	DYNC1I1	dynein, cytoplasmic, intermediate polypeptide 1	10 ± 2*	3 ± 1	1 ± 1
	HLADRA#	major histocompatibility complex, class II, DR alpha	1455 ± 574*	45 ± 18	1 ± 0
	HLADRB#	major histocompatibility complex, class II, DR beta	990 ± 353*	43 ± 22	1 ± 0
	TFPI2#	tissue factor pathway inhibitor 2	7 ± 2*	13 ± 6	1 ± 1
	TGM2	transglutaminase 2	46 ± 16*	7 ± 3	1 ± 0
	GMFG	glia maturation factor, gamma	3 ± 2	4 ± 1*	1 ± 0
	IGFBP5	insulin-like growth factor binding protein 5	5 ± 2	26 ± 5*	1 ± 0
	MCTP2	multiple C2-domains with two transmembrane regions 2	3 ± 1	23 ± 6*	1 ± 0
	PLAU	plasminogen activator, urokinase	4 ± 1	7 ± 1*	1 ± 0
B	MCAM	melanoma cell adhesion molecule	36 ± 2*	1 ± 0	1 ± 0
C	CCND1	cyclin D1	1 ± 1	3 ± 1*	1 ± 0
	EDG2	endothelial differentiation, lysophosphatidic acid G-protein-coupled receptor, 2	1 ± 0	4 ± 1*	1 ± 0
	F2R	coagulation factor II (thrombin) receptor	1 ± 0	12 ± 3*	1 ± 0
	LEPR	leptin receptor	3 ± 2	31 ± 9*	1 ± 0

RNA was isolated from BMSC cultures at passage 5–8. Relative mRNA levels were determined by real time quantitative RT-PCR, and were normalized in I-BMSC ($n = 14$) and A-BMSC ($n = 6$) against those obtained with 6 fibroblasts. Values are averages ± SEM for 6 ~ 14 cultures.

*Statistically significant $*p < 0.05$.

#Previously reported genes.[12]

Underlines: We selected these markers for optimal assays, considering the effects of *in vivo* location of BMSC and passage, magnitude of increase in expression levels and inter-individual differences (see Discussion).

Group B gene ($n = 1$) showed significantly higher expression levels in I-BMSCs than in fibroblasts, whereas the expression levels in A-BMSCs were similar to those in fibroblasts, so group B gene was considered to be a specific marker for I-BMSCs.

Group C genes ($n = 4$) showed significantly higher expression levels in A-BMSCs than in fibroblasts, whereas their expression levels in I-BMSCs were similar to those in fibroblasts, so group C genes were considered to be specific markers for A-BMSCs.

Expression of marker genes in F-BMSCs and T-BMSCs

Next, we examined expression levels of these markers in long-bone BMSCs (F-BMSCs and T-BMSCs). Figure 2 shows the mRNA levels of marker genes in F-BMSCs, T-BMSCs, I-BMSCs, and A-BMSCs in comparison with those in fibroblasts. The expression levels of group A-1 and A-2 genes in F-BMSCs and T-BMSCs were higher than those in fibroblasts, and many of these were comparable

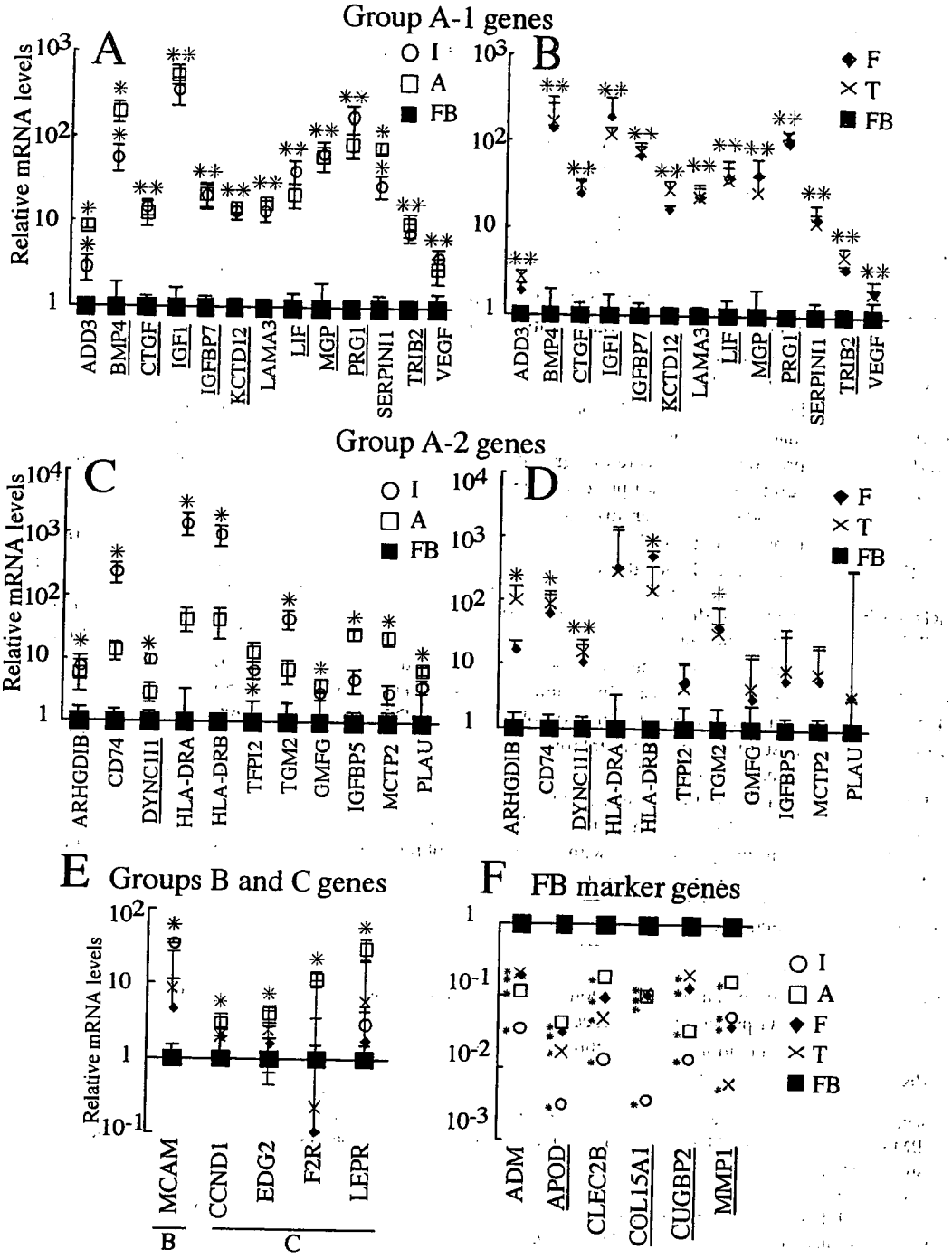

FIG. 2. The expression levels of the candidate marker genes in confluent cultures of I-BMSCs (I, $n = 14$), A-BMSCs (A, $n = 6$), F-BMSCs (F, $n = 3$), and T-BMSCs (T, $n = 3$) relative to those in fibroblasts (FB, $n = 6$) were determined by quantitative RT-PCR using low-density array cards. RNA was isolated from BMSC cultures at passages 5–8. Panels (**A**) and (**C**) show the mRNA levels of group A genes in I-BMSCs and A-BMSCs, and panels (**B**) and (**D**) show those in F-BMSCs and T-BMSCs. The expression levels of most marker genes were significantly different ($*p < 0.05$) from those in fibroblasts. The expression levels of group A-2 genes were higher (>3-fold) than those in fibroblasts (**C**, **D**). The expression levels of CD74, HLA-DRB and DYC111 in I-BMSCs and F-BMSCs were significantly different from those in fibroblasts (**C**, **D**). The expression levels of ARHGDIB, TGM2 and DYC111 in I-BMSCs and T-BMSCs were significantly different from those in fibroblasts (**C**, **D**). The expression levels of GMFG, IGFBP5, MCTP2 and PLAU in A-BMSCs were significantly different from those in fibroblasts (**C**, **D**). The expression level of MCAM in I-BMSCs was significantly different from those in fibroblasts (**E**). The expression levels of group C genes in A-BMSCs were significantly different from those in fibroblasts (**C**, **D**). The mRNA levels of groups B and C are shown in panel (**E**), and those of fibroblast markers are shown in panel (**F**). Underlined are the markers we had selected for optimal assays, considering the effects of *in vivo* location of BMSCs and passage number, magnitude of increase in expression levels, and interindividual differences (see "Discussion" section).

to those in I-BMSCs and A-BMSCs, proving that group A genes are common markers for BMSCs from various bones.

The mRNA levels of melanoma cell adhesion molecule (MCAM) (group B) in F-BMSCs and T-BMSCs were lower than those in I-BMSCs, but higher than those in A-BMSCs or fibroblasts (Fig. 2). The mRNA levels of thrombin receptor (F2R) and leptin receptor (LEPR) (group C) in F-BMSCs and T-BMSCs were similar to those in I-BMSCs, and lower than those in A-BMSCs (Fig. 2), suggesting that the gene expression profile in long-bone BMSCs is similar to that in I-BMSCs, but differs from that in A-BMSCs.

In previous studies, we showed that mRNA levels of adrenomedullin (ADM), apolipoprotein D (APOD), C-type lectin superfamily member 2 (CLEC2B), collagen type XV α1 (COL15A1), CUG triplet repeat RNA-binding protein 2 (CUGBP2), and MMP1 were lower in A-BMSCs or I-BMSCs than in fibroblasts.[27] These mRNA levels also proved to be lower in F-BMSCs and T-BMSCs than in fibroblasts (Fig. 2).

In Figure 2, sample numbers were different among A-BMSCs ($n=6$), I-BMSCs ($n=14$), T-BMSCs ($n=3$), F-BMSCs ($n=3$), skin fibroblasts ($n=5$), and gum fibroblasts ($n=1$). To reduce this variability, we examined the expression levels of marker genes in an additional six A-BMSC lines and an additional three gum fibroblast lines. The sample numbers had little effect on the expression levels of these genes (data not shown).

Effects of passage and age on marker gene expression levels

If the passage of BMSC cultures markedly affects gene expression levels of marker genes, such markers may be less useful in clinical studies, so we examined the marker gene expression levels as a function of the passage number (Fig. 3). In this study, the passage number markedly altered the expression of several marker genes, including serine (or cysteine) proteinase inhibitor, clade I, member 1 (SERPINI1); CD74 antigen (CD74); and transglutaminase 2 (TGM2). The marker genes in Figure 3B did not always show significantly higher expression levels in I-BMSCs than in fibroblasts at some passage numbers. However, LIF, insulin-like growth factor 1 (IGF1), proteoglycan 1 (PRG1), matrix Gla protein (MGP), bone morphogenetic protein 4 (BMP4), connective tissue growth factor (CTGF), potassium channel tetramerization domain containing 12 (KCTD12), insulin-like growth factor binding protein 7 (IGFBP7), tribbles homolog 2 (TRIB2), VEGF, and dynein (DYNC1I1) showed higher expression levels in I-BMSCs than in fibroblasts, irrespective of the passage number (Fig. 3A). In contrast, the expression levels of fibroblast markers were consistently lower in BMSCs than in fibroblasts, irrespective of the passage number (Fig. 3C).

To confirm the usefulness of the markers, we examined the effect of age on the marker gene expression levels in I-BMSCs from 14 individual lines. No significant differences in the expression levels of marker genes were observed between young I-BMSC lines (I-BMSC-y, $n=7$, age 18–39 years) and old I-BMSC lines (I-BMSC-o, $n=7$, age 53–81 years) (upper panel, Fig. 4), and between young A-BMSC lines (A-BMSC-y, $n=6$, age 19–25 years) and old A-BMSC lines (A-BMSC-o, $n=6$, age 43–63 years) (lower panel).

Use of the marker genes in clinical studies

We are now doing clinical studies on regenerative medicine for periodontal diseases using autologous BMSCs.[19,32] In a previous report, we showed that SERPINI1, tissue factor pathway inhibitor 2 (TFPI2), major histocompatibility complex class II DR alpha (HLADRA), major histocompatibility complex class II DR beta (HLADRB), and CD74 expression levels were higher in BMSC lines from a few patients than in fibroblasts,[27] but it was unclear whether these and the other common markers would be useful in clinical studies for a large number of patients. In the present study, we compared mRNA levels of 13 genes of group A-1, 7 genes of group A-2, and 1 gene of group B in I-BMSC lines from patient 1 (age 63 years, male), patient 2 (39 years, male), patient 3 (64 years, female), patient 4 (46 years, female), patient 5 (25 years, male), patient 6 (56 years, female), patient 7 (52 years, female), patient 8 (22 years, male), and patient 9 (40 years, female) with those in fibroblast lines (Table 2). We found that LIF, IGF1, PRG1, MGP, BMP4, CTGF, KCTD12, IGFBP7, TRIB2, HLADRB, HLADRA, CD74, TGM2, DYNC1I1, and MCAM expression levels were consistently much higher (greater than fourfold) in the BMSC lines than in fibroblasts, although HLADRB and HLADRA levels showed very large interindividual differences (>100-fold). Adducin 3 (ADD3), SERPINI1, Rho GDP dissociation inhibitor beta (ARHGDIB), and TFPI2 expression levels were not always higher in patients' BMSCs than in fibroblasts, and laminin alpha 3 (LAMA3) and VEGF expression levels in some BMSC lines were only two- to fourfold higher than in fibroblasts.

In addition, six fibroblast markers also proved useful for quality examination of patients' BMSCs (Table 2). APOD, COL15A1, CUGBP2, and MMP1 levels, in particular, were much lower (<5%) in all BMSC lines than in fibroblasts, so these may be reliable negative markers for BMSCs.

Secreted levels of several markers

Since enzyme-linked immunosorbent assay (ELISA) provides verification that differential gene expression translates to changes in protein levels, we examined the secreted levels of several markers in I-BMSC and fibroblast cultures by ELISA (Fig. 5). We found that the LIF and VEGF levels in I-BMSC cultures were consistently higher than those in fibroblast cultures, whereas the pro-MMP1 levels in fibroblast cultures were consistently higher than those in I-BMSC cultures.

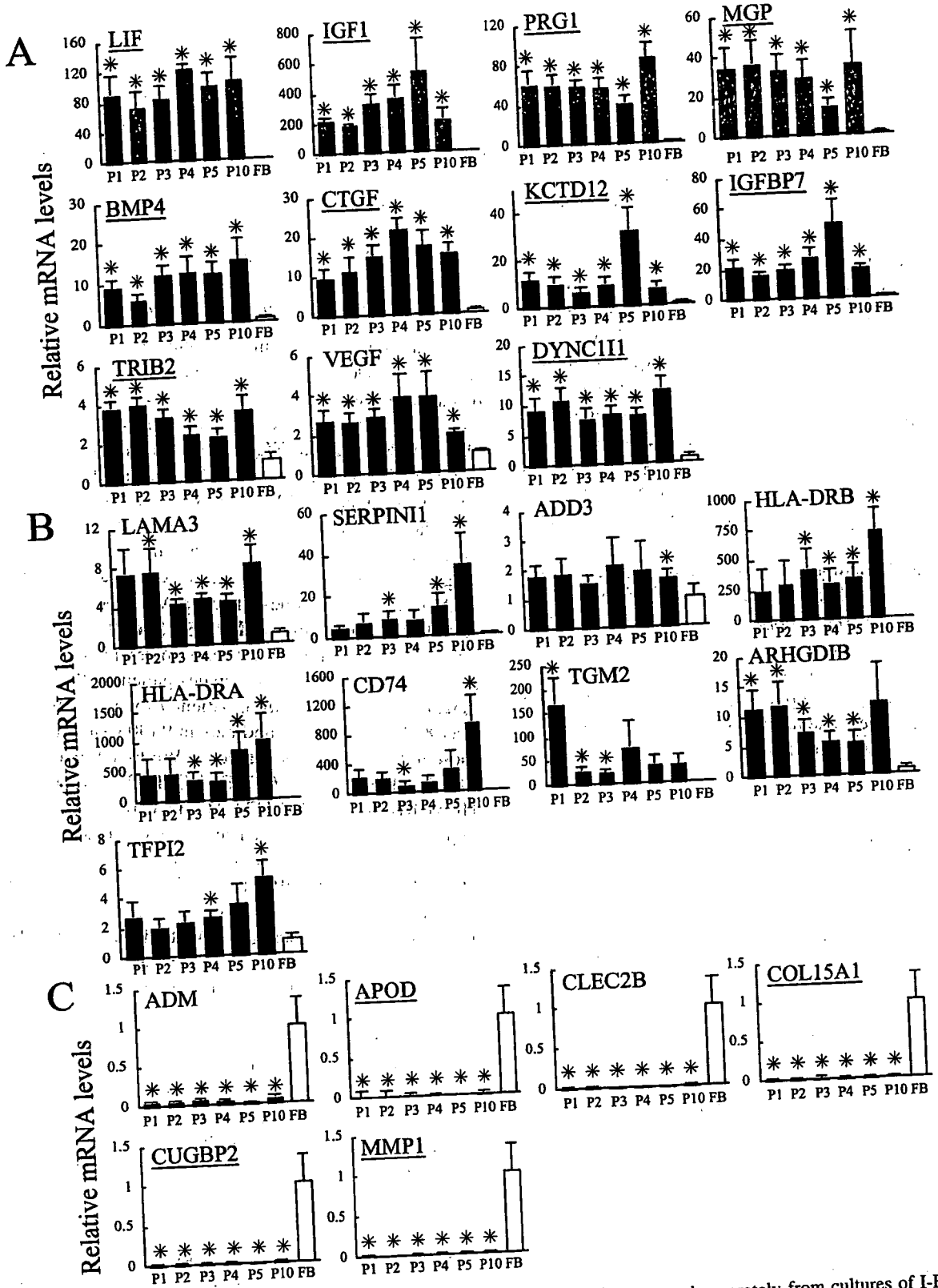

FIG. 3. Effect of passage number on marker gene expression levels. RNA was harvested separately from cultures of I-BMSC lines from four donors and fibroblast lines from four donors. (**A**) Most group A genes showed consistently higher expression levels in four I-BMSC lines than in four standard fibroblast lines (FB, open columns) at passages 1, 2, 3, 4, 5, and 10 ($*p < 0.05$). (**B**) Some group A genes showed significantly higher expression levels in four I-BMSC lines than in four fibroblast lines only at some passage numbers ($*p < 0.05$). (**C**) The expression levels of fibroblast marker genes were consistently lower in four I-BMSC lines than in four fibroblast lines at passages 1, 2, 3, 4, 5, and 10 ($*p < 0.05$). The values are mean ± SEM for four cultures. Underlined are the markers we had selected for optimal assays, considering the effects of *in vivo* location of BMSCs and passage number, magnitude of increase in expression levels, and interindividual differences (see "Discussion" section).

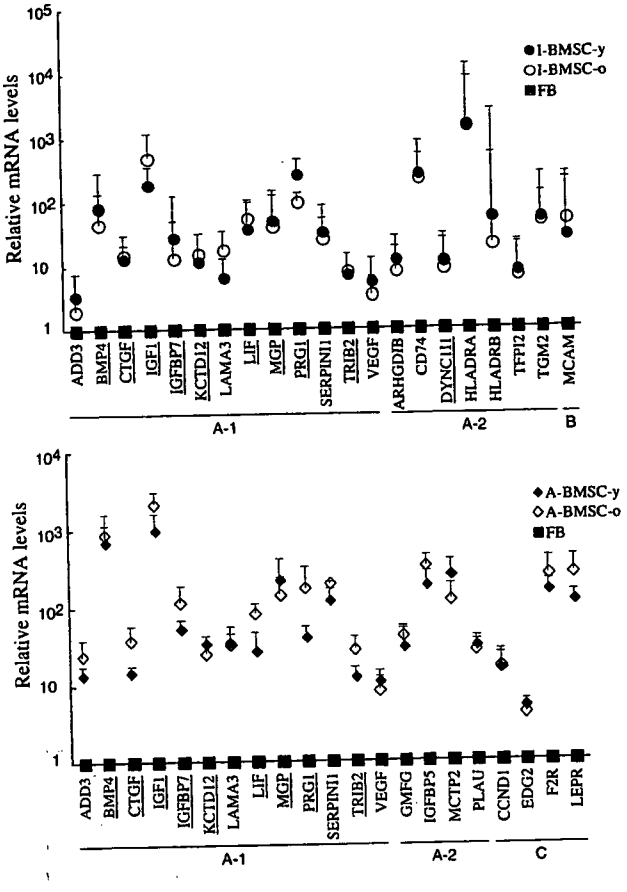

FIG. 4. Effect of age on marker gene expression levels. The expression levels (mean ± SEM) of marker genes in young I-BMSCs (closed circles, $n = 7$, age 18–39 years) and old I-BMSCs (open circles, $n = 7$, age 53–81 years) relative to standard fibroblasts (closed squares, $n = 6$, age 17–47 years), along with young A-BMSCs (closed diamonds, $n = 6$, age 19–25 years) and old A-BMSCs (open diamonds, $n = 6$, age 43–63 years), were determined. RNA was isolated from BMSC cultures at passages 5–8. No marker genes showed any significant difference between young I-BMSCs and old I-BMSCs or between young A-BMSCs and old A-BMSCs. Underlined are the markers we had selected for optimal assays, considering the effects of *in vivo* location of BMSCs and passage number, magnitude of increase in expression levels, and interindividual differences (see "Discussion" section).

DISCUSSION

Identity and purity of transplantable cells are essential factors for the efficacy and evaluation of tissue engineering and cell therapy, but optimal assays for *ex vivo*–expanded BMSCs have not been established. While several DNA microarray studies have revealed the gene expression profile of BMSCs,[33–40] and some studies have identified a number of BMSC markers that may distinguish BMSCs from fibroblasts,[27,33,34] it remained unclear whether these would be reliable markers in clinical studies, since previous studies had quantified expression of a small number of candidate marker genes with a small number of examined BMSC lines. It also remained unknown whether these markers were common for BMSCs from various bones. Different microenvironments, shapes, and sizes of various bones may affect the expression of BMSC markers, and "some" BMSC markers may depend upon the *in vivo* location of bone.

In this study, we demonstrated that the differentiation potential of F-BMSCs and T-BMSCs (long-bone BMSCs) is similar to that of I-BMSCs, but different from that of A-BMSCs (Fig. 1). Nonetheless, all BMSC lines expressed numerous common markers at similar mRNA levels, whereas several markers showed discrete expression levels between A-BMSCs and other BMSCs (Fig. 2). The distinct gene expression profile of A-BMSCs could be accounted for by origin: alveolar/jaw bone originates in the ectoderm (neural crest), whereas the ilium, tibia, and femur originate in the mesoderm.

We referred to stromal cells, which were isolated from bone marrow aspirates, adhered on the substrate, and proliferated in monolayer cultures, as BMSCs, although these cells are often called mesenchymal stem cells. The definition of mesenchymal stem cells is controversial, but we define mesenchymal stem cells as stromal cells that have multilineage differentiation potential, including osteogenic, chondrogenic, and adipogenic potentials. I-BMSCs, T-BMSCs, and F-BMSCs showed this multipotentiality, indicating that these cells were indeed mesenchymal stem cells, whereas A-BMSCs had poor chondrogenic and adipogenic potentials. The reason for this discrepancy is unknown, but in the presence of common markers for BMSCs, the chondrogenic and adipogenic potentials of A-BMSCs may be suppressed by some genes *in vivo* location dependently.

In this study, we found that many markers were common for all BMSCs, while only one marker (MCAM) was positive for I-BMSCs, T-BMSCs, and F-BMSCs, and negative for A-BMSCs. The expression of MCAM may be linked with multipotentiality or could be suppressed in some bones—irrespective of multipotentiality. This point needs further investigation. However, the common markers will be useful for identification of BMSCs with osteogenic potential, and the expression of these markers did not suppress the multilineage differentiation potential of I-BMSCs, T-BMSCs, or F-BMSCs. Since BMSCs from various bones will be used for treatment of various diseases, common markers may be useful in routine tests. In addition, some markers that are directly linked with multipotentiality may be useful in the future. The identification of markers functionally linked with multipotentiality will be an important issue in future studies.

Most of the common and *in vivo* location–dependent markers were involved in signal transduction by growth factors/cytokines (IGF1, LIF, BMP4, VEGF, CTGF, IGFBP5, IGFBP7, F2R, LEPR, etc.) or in remodeling of extracellular matrix (LAMA3, MGP, PRG1, SERPINI1, TGM2, TFPI2, etc.). Whether the expression levels of these markers are related to the differentiation potential of BMSCs will also be investigated in the future.

TABLE 2. MESSENGER RNA LEVELS OF MARKER GENES IN *EX VIVO* EXPANDED BMSC POPULATIONS BEFORE TRANSPLANTATION

		Pt. 1 *P1*	*Pt. 2* *P2*	*Pt. 3* *P1*	*Pt. 4* *P2*	*Pt. 5* *P1*	*Pt. 6* *P2*	*Pt. 7* *P2*	*Pt. 8* *P2*	*Pt. 9* *P2*	*FB (n=6)*
Group	*Gene symbol*	*Relative mRNA levels*									
A-1	LIF	70	22	239	68	221	1330	265	47	195	1±1
	IGF1	111	146	131	174	81	260	453	548	71	1±1
	PRG1	63	147	151	156	62	142	134	110	92	1±0
	MGP	51	41	52	54	17	69	221	12	327	1±1
	BMP4	158	8	18	11	41	34	60	6	53	1±1
	CTGF	10	29	29	9	15	14	16	18	16	1±0
	KCTD12	26	13	9	15	7	19	12	14	20	1±0
	LAMA3	33	4	12	5	8	16	29	13	16	1±0
	IGFBP7	9	8	15	15	19	5	11	10	19	1±1
	SERPINI1	41	4	6	4	2	4	4	11	4	1±1
	TRIB2	10	7	8	10	8	7	7	9	11	1±0
	VEGF	3	4	8	5	3	9	5	13	2	1±0
	ADD3	2	2	2	2	1	2	2	2	2	1±1
A-2	HLADRB	15	502	3394	28	5124	1002	996	83	749	1±0
	HLADRA	264	512	3279	4429	1064	160	146	37	79	1±0
	CD74	85	187	473	823	170	462	360	16	104	1±1
	TGM2	33	133	29	185	55	34	49	38	105	1±1
	DYNC1I1	7	6	7	10	4	12	9	14	9	1±1
	ARHGDIB	3	3	29	3	10	19	3	1	5	1±1
	TFPI2	4	2	8	13	11	13	8	3	6	1±0
B	MCAM	12	16	40	74	21	84	57	69	24	1±0
FB marker genes	ADM	1×10^{-3}	3×10^{-3}	2×10^{-3}	1×10^{-3}	3×10^{-3}	1×10^{-3}	5×10^{-3}	3×10^{-3}	3×10^{-3}	1±0
	APOD	9×10^{-3}	6×10^{-3}	1×10^{-3}	3×10^{-3}	6×10^{-4}	7×10^{-4}	1×10^{-3}	5×10^{-3}	7×10^{-3}	1±0
	CLEC2B	2×10^{-3}	8×10^{-3}	4×10^{-3}	2×10^{-3}	5×10^{-3}	4×10^{-3}	1×10^{-3}	1×10^{-2}	4×10^{-3}	1±0
	COL15A1	9×10^{-3}	3×10^{-2}	3×10^{-3}	7×10^{-4}	2×10^{-4}	7×10^{-3}	4×10^{-4}	1×10^{-2}	4×10^{-4}	1±0
	CUGBP2	3×10^{-2}	2×10^{-2}	3×10^{-2}	3×10^{-2}	2×10^{-2}	3×10^{-2}	3×10^{-2}	5×10^{-2}	6×10^{-2}	1±0
	MMP1	2×10^{-2}	8×10^{-3}	1×10^{-2}	1×10^{-2}	2×10^{-1}	6×10^{-2}	8×10^{-3}	8×10^{-3}	8×10^{-3}	1±0

Relative mRNA levels in BMSC cultures at passage 1 or 2 (P1 or P2) were determined by real time quantitative RT-PCR, and were normalized in BMSC lines from 9 patients (Pt.1–Pt.9) against the values obtained with 6 fibroblast lines.

Abbreviations: FB, Fibroblast; P, Passage numbers.

Underlines: We selected these markers for optimal assays, considering the effects of *in vivo* location of BMSC and passage, magnitude of increase in expression levels and inter-individual differences (see Discussion).

We first identified the above markers from BMSC cultures at the fifth to eighth passage, but we confirmed, using nine patients' BMSC lines, that the mRNA levels of the marker genes were also much higher (greater than fourfold) in BMSCs at the first or second passage than in fibroblasts, except for ADD3, SERPINI1, ARHGDIB, and TFPI2; LAMA3 and VEGF expression levels in some BMSC lines were only two- to fourfold higher than in fibroblasts (Table 2). In subsequent studies, a passage-dependent difference was observed for several markers (Fig. 3), but LIF, IGF1, PRG1, MGP, BMP4, CTGF, KCTD12, IGFBP7, TRIB2, and DYNC1I1 showed higher expression levels in BMSCs, irrespective of the passage number, than in fibroblasts (Fig. 3A); these may be reliable markers for *ex vivo*–expanded BMSCs. On the other hand, LAMA3, SERPINI1, ADD3, HLADRB, HLADRA, CD74, TGM2, ARHGDIB, and TFPI2 did not show consistently higher expression levels in BMSCs than in fibroblasts at some passage numbers, and HLADRA and HLADRB showed very large interindividual differences (>100-fold), so these are probably not reliable markers (Fig. 3B and Table 2). Proliferation, senescence, or adaptation to culture conditions may have affected the expression of some markers, passage number dependently. We also showed that donor age had little effect on the expression levels of the marker genes in BMSCs (Fig. 4), which will be of great importance in clinical studies for patients of various ages.

We selected BMSC markers from many candidates for optimal assays, considering interindividual differences (Table 2), magnitude of increase in expression levels relative to fibroblasts (Table 2), and the effects of passage (Fig. 3) and *in vivo* location of BMSCs (Table 1 and Fig. 2). LIF, IGF1, PRG1, MGP, BMP4, CTGF, KCTD12, IGFBP7, TRIB2, and DYNC1I1 proved to be reliable positive mark-

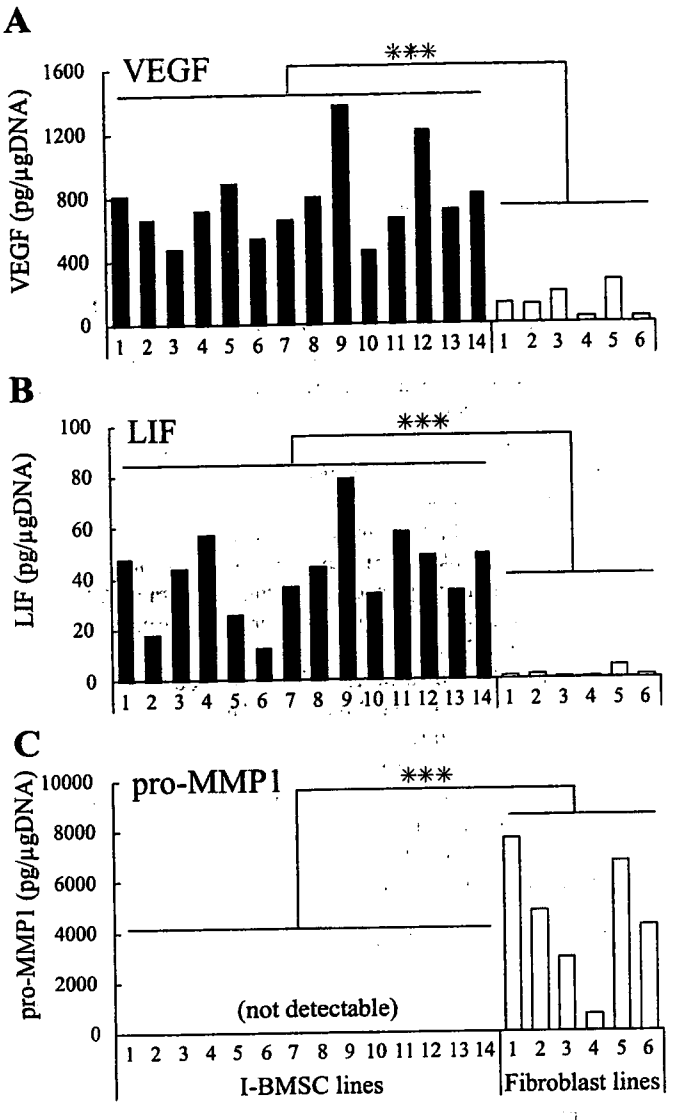

FIG. 5. Quantification of marker protein levels by ELISA. (**A**) VEGF, (**B**) LIF, and (**C**) pro-MMP1 levels in the culture medium of I-BMSC lines (closed columns) or fibroblast lines (open columns) were determined by ELISA. The media were isolated from BMSC cultures at passages 5–8. The secreted protein levels were significantly different (***$p < 0.001$) between BMSCs and fibroblast lines.

ers for BMSCs, whereas APOD, COL15A1, CUGBP2, and MMP1 were reliable negative markers (underlined genes in Tables 1 and 2, and Figs. 2–4). The positive and negative marker sets should thus be combined in a routine test. We also found that LIF, VEGF, and pro-MMP1, as determined by ELISA, were useful in distinguishing BMSCs from fibroblasts (Fig. 5). A combination of ELISA and RT-PCR may provide more accurate results.

It is interesting to compare BMSC markers identified in this study with those in other studies.[33,34,40] Wagner *et al.*[33] selected 25 marker genes that were expressed at higher levels in bone marrow mesenchymal stem cells, adipose tissue–derived mesenchymal stem cells, and cord blood–derived mesenchymal stem cells than in fibroblasts. Of the 25 genes, 17 were examined in our DNA microarray analyses, but Wagner's positive mesenchymal stem cell markers did not show any significant difference in the present study, although MMP1 was a negative marker in both Wagner's and our studies. Brendel *et al.*[34] found that 21 genes were up-regulated in human BMSCs compared with fibroblasts, using DNA microarray containing 9,600 probes. Of the 21 genes, 12 genes were included in our DNA microarray probes, but Brendel's BMSC markers did not show any significant difference in the present study, except for IGFBP5: IGFBP5 and IGFBP7 were included in our BMSC-marker list (Table 1 and Fig. 2). In addition, Wagner and Brendel identified negative markers, which were expressed at higher levels in fibroblasts than in BMSCs or mesenchymal stem cells, but these negative markers were not included in our list of fibroblast markers except for MMP1 (Table 2 and Fig. 2).

These varying results may be due to different chips, culture conditions, and cells used: Wagner used HS68 fibroblasts, whereas we used gum-derived and skin-derived fibroblasts. In addition, Wagner searched for common makers in various mesenchymal stem cell lines from bone marrow, adipose tissue, and cord blood, whereas we searched for common markers in bone marrow BMSC lines from various bones. Neither Wagner nor Brendel confirmed the differential expression of all candidate genes by quantitative RT-PCR, but in our experience, DNA microarray analysis often produces false positives and false negatives.

In preliminary studies with GeneChip (U133 plus 2.0 Array, Affimetrix) containing ~54,000 probes, we extended our studies of BMSC markers and found that some of Wagner's markers, including PLOD2, CSPG2, HOXA5, and TM4SF1, were higher in I-BMSC lines than in fibroblast lines, and some of Brendel's markers, including PLOD2, IGFBP5, ABLIM1, COL4A2, DLX5, EYA2, ID3, and IRX3, were also higher in I-BMSC lines than in fibroblast lines (data not shown). In addition to the markers listed in Tables 1 and 2, these may also be useful for identification of BMSCs. Reproducibility in different laboratories and further characterization of the additional markers may prove useful in the future.

Recently, Song *et al.*[40] identified a number of "stemness" genes that might be essential to maintain adult stem cell multipotency, and "differentiation" genes that might be essential to maintain the differentiation state. The "stemness" genes were expressed in undifferentiated BMSCs and dedifferentiated mesenchymal stem-like cells that were obtained from cultures of BMSC-derived osteoblasts, BMSC-derived chondrocytes, or BMSC-derived adipocytes. These genes were down-regulated in BMSC-derived osteoblasts, BMSC-derived chondrocytes, and/or BMSC-derived adipocytes. Song did not determine the expression levels of these genes in fibroblasts, but LIF, PRG1, TFPI2, MCTP2, and PLAU were commonly included in both their and our BMSC

marker lists, and MMP1 and COL15A1 were included in both their "differentiation" gene list and our negative BMSC marker list (Table 2). Song also examined the effects of siRNA against several marker genes on proliferation and differentiation of BMSCs, an approach that may promote studies on the functional aspects of BMSC markers.

In conclusion, we identified reliable markers for bone marrow BMSCs by real-time RT-PCR with low-density array cards, considering the effects of *in vivo* location of BMSCs and passage numbers, magnitude of increase in expression levels, and interindividual differences. We believe that these markers will be useful in a routine test for BMSCs in tissue engineering and cell therapy.

ACKNOWLEDGMENTS

This study was supported by a fund from Japan Science and Technology Agency, and that from National Institute of Health Sciences, Japan (Division of Medical Devices, T. Tsuchiya's group).

REFERENCES

1. Pittenger, M.F., Mackay, A.M., Beck, S.C., Jaiswal, R.K., Douglas, R., Mosca, J.D., Moorman, M.A., Simonetti, D.W., Craig, S., and Marshak, D.R. Multilinage potential of adult human mesenchymal stem cells. Science **284,** 143, 1999.
2. Caplan, A.I., and Bruder, S.P. Mesenchymal stem cells: building blocks for molecular medicine in the 21st century. Trends Mol. Med. **7,** 259, 2001.
3. Sekiya, I., Larson, B.L., Smith, J.R., Pochampally, R., Cui, J.G., and Prockop, D.J. Expansion of human adult stem cells from bone marrow stroma: conditions that maximize the yields of early progenitors and evaluate their quality. Stem Cells **20,** 530, 2002.
4. Makino, S., Fukuda, K., Miyoshi, S., Konishi, F., Kodama, H., Pan, J., Sono, M., Takahashi, T., Hori, S., Abe, H., Hata, J., Umezawa, A., and Ogawa, S. Cardiomyocytes can be generated from bone marrow stromal cells *in vitro*. J. Clin. Invest. **103,** 697, 1999.
5. Deans, R.J., and Moseley, A.B. Mesenchymal stem cells: biology and potential clinical uses. Exp. Hematol. **28,** 875, 2000.
6. Kopen, G.C., Prockop, D.J., and Phinney, D.G. Marrow stromal cells migrate throughout forebrain and cerebellum, and they differentiate into astrocyte after injection into neonatal mouse brains. Proc. Natl. Acad. Sci. USA **96,** 10711, 1999.
7. Horwitz, E.M., Prockop, D.J., Fitzpatrick, L.A., Koo, W.W., Gordon, P.L., Neel, M., Sussman, M., Orchard, P., Marx, J.C., Pyeritz, R.E., and Brenner, M.K. Transplantability and therapeutic effects of bone marrow-derived mesenchymal cells in children with osteogenesis imperfecta. Nat. Med. **5,** 309, 1999.
8. Quarto, R., Mastrogiacomo, M., Cancedda, R., Kutepov, S.M., Mukhachev, V., Lavroukov, A., Kon, E., and Marcacci, M. Repair of large bone defects with the use of autologous bone marrow stromal cells. N. Engl. J. Med. **344,** 385, 2001.
9. Tsutsumi, S., Shimazu, A., Miyazaki, K., Pan, H., Koike, C., Yoshida, E., Takagishi, K., and Kato, Y. Retention of multilineage differentiation potential of mesenchymal cells during proliferation in response of FGF. Biochem. Biophys. Res. Commun. **288,** 413, 2001.
10. Matsubara, T., Tsutsumi, S., Pan, H., Hiraoka, H., Oda, R., Nishimura, M., Kawaguchi, H., Nakamura, K., and Kato, Y. A new technique to expand human mesenchymal stem cells using basement membrane extracellular matrix. Biochem. Biophys. Res. Commun. **313,** 503, 2004.
11. Matsubara, T., Suardita, K., Ishii, M., Sugiyama, M., Igarashi, A., Oda, R., Nishimura, M., Saito, M., Nakagawa, K., Yamanaka, K., Miyazaki, K., Shimizu, M., Bhawal, U.K., Tsuji, K., Nakamura, K., and Kato, Y. Alveolar bone marrow as a cell source for regenerative medicine: differences between alveolar and iliac bone marrow stromal cells. J. Bone Miner. Res. **20,** 399, 2005.
12. Ohgushi, H., and Caplan, A.I. Stem cell technology and bioceramics: from cell to gene engineering. J. Biomed. Mater. Res. **48,** 913, 1999.
13. Hosseinkhani, H., Yamamoto, M., Inatsugu, Y., Hiraoka, Y., Inoue, S., Shimokawa, H., and Tabata, Y. Enhanced ectopic bone formation using a combination of plasmid DNA impregnation into 3-D scaffold and bioreactor perfusion culture. Biomaterials **27,** 1387, 2006.
14. Nishikawa, M., Ohgushi, H., Tamai, N., Osuga, K., Uemura, M., Yoshikawa, H., and Myoui, A. The effect of simulated microgravity by three-dimensional clinostat on bone tissue engineering. Cell Transplant. **14,** 829, 2005.
15. Wakitani, S., Imoto, K., Yamamoto, T., Saito, M., Murata, N., and Yoneda, M. Human autologous culture expanded bone marrow mesenchymal cell transplantation for repair of cartilage defects in osteoarthritic knees. Osteoarthr. Cartil. **10,** 199, 2002.
16. Shao, X., Goh, J.C., Hutmacher, D.W., Lee, E.H., and Zigang, G. Repair of large articular osteochondral defects using hybrid scaffolds and bone marrow-derived mesenchymal stem cells in a rabbit model. Tissue Eng. **12,** 1539, 2006.
17. Wang, T., Dang, G., Guo, Z., and Yang, M. Evaluation of autologous bone marrow mesenchymal stem cell—calcium phosphate ceramic composite for lumbar fusion in Rhesus monkey interbody fusion model. Tissue Eng. **11,** 1159, 2005.
18. Bensaid, W., Oudina, K., Viateau, V., Potier, E., Bousson, V., Blanchat, C., Sedel, L., Guillemin, G., and Petite, H. *De novo* reconstruction of functional bone by tissue engineering in the metatarsal sheep model. Tissue Eng. **11,** 814, 2005.
19. Kawaguchi, H., Hirachi, A., Hasegawa, N., Iwata, T., Hamaguchi, H., Shiba, H., Takata, T., Kato, Y., and Kurihara, H. Enhancement of periodontal tissue regeneration by transplantation of bone marrow mesenchymal stem cells. J. Periodontol. **75,** 1281, 2004.
20. Orii, H., Sotome, S., Chen, J., Wang, J., and Shinomiya, K. Beta-tricalcium phosphate (beta-TCP) graft combined with bone marrow stromal cells (MSCs) for posterolateral spine fusion. J. Med. Dent. Sci. **52,** 51, 2005.
21. Yamada, Y., Ueda, M., Naiki, T., Takahashi, M., Hata, K., and Nagasaka, T. Autogenous injectable bone for regeneration with mesenchymal stem cells and platelet-rich plasma: tissue-engineered bone regeneration. Tissue Eng. **10,** 955, 2004.
22. Morishita, T., Honoki, K., Ohgushi, H., Kotobuki, N., Matsushima, A., and Takakura, Y. Tissue engineering approach to the treatment of bone tumors: three cases of cultured bone

grafts derived from patients' mesenchymal stem cells. Artif. Organs **30,** 115, 2006.
23. Uematsu, K., Hattori, K., Ishimoto, Y., Yamauchi, J., Habata, T., Takakura, Y., Ohgushi, H., Fukuchi, T., and Sato, M. Cartilage regeneration using mesenchymal stem cells and a three-dimensional poly-lactic-glycolic acid (PLGA) scaffold. Biomaterials **26,** 4273, 2005.
24. Wayne, J.S., McDowell, C.L., Shields, K.J., and Tuan, R.S. *In vivo* response of polylactic acid-alginate scaffolds and bone marrow-derived cells for cartilage tissue engineering. Tissue Eng. **11,** 953, 2005.
25. Kalia, P., Blunn, G.W., Miller, J., Bhalla, A., Wiseman, M., and Coathup, M.J. Do autologous mesenchymal stem cells augment bone growth and contact to massive bone tumor implants? Tissue Eng. **12,** 1617, 2006.
26. Weinand, C., Gupta, R., Huang, A.Y., Weinberg, E., Madisch, I., Qudsi, R.A., Neville, C.M., Pomerantseva, I., and Vacanti, J.P. Comparison of hydrogels in the *in vivo* formation of tissue-engineered bone using mesenchymal stem cells and beta-tricalcium phosphate. Tissue Eng. **13,** 757, 2007.
27. Ishii, M., Koike, C., Igarashi, A., Yamanaka, K., Pan, H., Higashi, Y., Kawaguchi, H., Sugiyama, M., Kamata, N., Iwata, T., Matsubara, T., Nakamura, K., Kurihara, H., Tsuji, K., and Kato, Y. Molecular markers distinguish bone marrow mesenchymal stem cells from fibroblasts. Biochem. Biophys. Res. Commun. **332,** 297, 2005.
28. Kawahara, K., and Shimazu, A. Expression and intracellular localization of progesterone receptors in cultured human gingival fibroblasts. J. Periodontal Res. **38,** 242, 2003.
29. Gitelman, H.J. An improved automated procedure for the determination of calcium in biological specimens. Anal. Biochem. **18,** 521, 1967.
30. Farndale, R.W., Sayers, C.A., and Barrett, A.J. A direct spectrophotometric microassay for sulfated glycosaminoglycans in cartilage cultures. Connect. Tissue Res. **9,** 247, 1982.
31. Guo, W., Choi, J.K., Kirkland, J.L., Corkey, B.E., and Hamilton, J.A. Esterification of free fatty acids in adipocytes: a comparison between octanoate and oleate. Biochem. J. **349,** 463, 2000.
32. Mizuno, N., Shiba, H., Ozeki, Y., Mouri, Y., Niitani, M., Inui, T., Hayashi, H., Suzuki, K., Tanaka, S., Kawaguchi H., and Kurihara, H. Human autologous serum obtained using a completely closed bag system as a substitute for fetal calf serum in human mesenchymal stem cell cultures. Cell Biol. Int. **30,** 521, 2006.
33. Wagner, W., Wein, F., Seckinger, A., Frankhauser, M., Wirkner, U., Krause, U., Blake, J., Schwager, C., Eckstein, V., Ansorge, W., and Ho, A.D. Comparative characteristics of mesenchymal stem cells from human bone marrow, adipose tissue, and umbilical cord blood. Exp. Hematol. **33,** 1402, 2005.
34. Brendel, C., Kuklick, L., Hartmann, O., Kim, T.D., Boudriot, U., Schwell, D., and Neubauer, A. Distinct gene expression profile of human mesenchymal stem cells in comparison to skin fibroblasts employing cDNA microarray analysis of 9600 genes. Gene Expr. **12,** 245, 2005.
35. Jeong, J.A., Hong, S.H., Gang, E.J., Ahn, C., Hwang, S.H., Yang, I.H., Han, H., and Kim, H. Differential gene expression profiling of human umbilical cord blood-derived mesenchymal stem cells by DNA microarray. Stem Cells **23,** 584, 2005.
36. Shahdadfar, A., Fronsdal, K., Haug, T., Reinholt, F.P., and Brinchmann, J.E. *In vitro* expansion of human mesenchymal stem cells: choice of serum is a determinant of cell proliferation, differentiation, gene expression, and transcriptome stability. Stem Cells **23,** 1357, 2005.
37. Wagner, W., Wein, F., Seckinger, A., Frankhauser, M., Wirkner, U., Krause, U., Blake, J., Schwager, C., Eckstein, V., Ansorge, W., and Ho, A.D. Comparative characteristics of mesenchymal stem cells from human bone marrow, adipose tissue, and umbilical cord blood. Exp. Hematol. **33,** 1402, 2005.
38. Kim, C.G., Lee, J.J., Jung, D.Y., Jeon, J., Heo, H.S., Kang, H.C., Shin, J.H., Cho, Y.S., Cha, K.J., Kim, C.G., Do, B.R., Kim, K.S., and Kim, H.S. Profiling of differentially expressed genes in human stem cells by cDNA microarray. Mol. Cells **21,** 343, 2006.
39. Yamada, Y., Fujimoto, A., Ito, A., Yoshimi, R., and Ueda, M. Cluster analysis and gene expression profiles: a cDNA microarray system-based comparison between human dental pulp stem cells (hDPSCs) and human mesenchymal stem cells (hMSCs) for tissue engineering cell therapy. Biomaterials **27,** 3766, 2006.
40. Song, L., Webb, N.E., Song, Y., and Tuan, R.S. Identification and functional analysis of candidate genes regulating mesenchymal stem cell self-renewal and multipotency. Stem Cells **24,** 1707, 2006.

Address reprint requests to:
Yukio Kato, D.D.S., Ph.D.
Department of Dental and Medical Biochemistry
Graduate School of Biomedical Sciences
Hiroshima University
1-2-3 Kasumi, Minami-Ku
Hiroshima 734-8553
Japan

E-mail: ykato@hiroshima-u.ac.jp

Transforming Growth Factor-β Promotes Survival of Mammary Carcinoma Cells through Induction of Antiapoptotic Transcription Factor DEC1

Shogo Ehata,[1,2,3] Aki Hanyu,[1] Makoto Hayashi,[1] Hiroyuki Aburatani,[4] Yukio Kato,[5] Makoto Fujime,[2] Masao Saitoh,[3] Keiji Miyazawa,[3] Takeshi Imamura,[1] and Kohei Miyazono[1,3]

[1]Department of Biochemistry, Cancer Institute of the Japanese Foundation for Cancer Research; [2]Department of Urology, Graduate School of Medicine, Juntendo University; [3]Department of Molecular Pathology, Graduate School of Medicine and [4]Genome Science Division, Research Center for Advanced Science and Technology, University of Tokyo, Tokyo, Japan and [5]Department of Dental and Medical Biochemistry, Graduate School of Biomedical Sciences, Hiroshima University, Hiroshima, Japan

Abstract

Transforming growth factor-β (TGF-β) signaling facilitates tumor growth and metastasis in advanced cancer. In the present study, we identified differentially expressed in chondrocytes 1 (DEC1, also known as SHARP2 and Stra13) as a downstream target of TGF-β signaling, which promotes the survival of breast cancer cells. In the mouse mammary carcinoma cell lines JygMC(A) and 4T1, the TGF-β type I receptor kinase inhibitors A-44-03 and SB431542 induced apoptosis of cells under serum-free conditions. Oligonucleotide microarray and real-time reverse transcription-PCR analyses revealed that TGF-β induced DEC1 in these cells, and the increase of DEC1 was suppressed by the TGF-β type I receptor kinase inhibitors as well as by expression of dominant-negative TGF-β type II receptor. Overexpression of DEC1 prevented the apoptosis of JygMC(A) cells induced by A-44-03, and knockdown of endogenous DEC1 abrogated TGF-β–promoted cell survival. Moreover, a dominant-negative mutant of DEC1 prevented lung and liver metastasis of JygMC(A) cells *in vivo*. Our observations thus provide new insights into the molecular mechanisms governing TGF-β–mediated cell survival and metastasis of cancer. [Cancer Res 2007;67(20):9694–703]

Introduction

Apoptosis is an important mechanism of negative regulation of cancer development and metastasis (1). During the process of metastasis, apoptosis occurs through various mechanisms; after the detachment of tumor cells from the extracellular matrix and the neighboring cells at primary tumor sites, forms of cell death known as anoikis and amorphosis occur. In the bloodstream, cell death occurs through immune surveillance and/or destruction by mechanical stress. At sites of secondary metastasis, cell death occurs after extravasation during the phase of formation of micrometastasis. These findings suggest that the metastatic potential of cancer cells is closely associated to their resistance to apoptosis.

Transforming growth factor-β (TGF-β) is a multifunctional cytokine that regulates the growth, differentiation, and apoptosis of various types of cells. TGF-β transduces signals through two distinct serine-threonine kinase receptors, termed type I (TβR-I) and type II (TβR-II). TβR-I is activated by TβR-II on ligand binding and transduces signals through various proteins, of which Smad proteins are the major signal transducers for TGF-β (2, 3). Activated TβR-I phosphorylates receptor-regulated Smads (R-Smads; i.e., Smad2 and Smad3), which interact with common mediator Smad (Smad4) and translocate to the nucleus. Nuclear Smad complexes bind to various transcription factors and transcriptional coactivators and regulate transcription of target genes. Transcriptional corepressors, including c-Ski and SnoN, inhibit TGF-β signaling through interaction with Smad complexes. Inhibitory Smads, including Smad6 and Smad7, are induced by TGF-β and bone morphogenetic proteins (BMP), bind to type I receptors, and prevent phosphorylation of R-Smads, resulting in inhibition of TGF-β family signaling.

TGF-β exerts both inhibitory and stimulatory effects on the progression of tumors (4, 5). In early stages of carcinogenesis, TGF-β serves as a tumor suppressor through inhibition of cell growth. Thus, mutations of signal components of TGF-β, including TβR-II and Smad4, have been reported to be responsible for progression of certain gastrointestinal tumors (6, 7). However, some tumor cells escape the growth inhibition induced by TGF-β, and TGF-β facilitates the progression and metastasis of tumors in advanced stages of cancer. TGF-β induces epithelial-to-mesenchymal transdifferentiation (EMT) in mammary epithelial cells. TGF-β also acts on the tumor microenvironment, where it stimulates angiogenesis and tissue fibrosis and causes local and systemic immunosuppression, leading to progression and metastasis of tumors.

TGF-β induces apoptosis of various types of cells, and the mechanisms of TGF-β–induced apoptosis have been extensively studied. Smad proteins play critical roles in execution of TGF-β–induced death in certain types of cells (8). Several genes regulated by Smad transcriptional complexes have been reported to be involved in TGF-β–mediated apoptosis, including *DAP-kinase*, *SHIP*, and *GADD45β* (8). In addition, certain molecules including the adaptor protein Daxx have been reported to be directly activated by TβR-II and to induce cell death through activation of c-Jun NH_2-terminal kinase (9). Most of these molecules regulate the expression of members of the Bcl-2 family and activate various caspases. On the other hand, it is becoming evident that TGF-β

Note: Supplementary data for this article are available at Cancer Research Online (http://cancerres.aacrjournals.org/).

Requests for reprints: Kohei Miyazono, Department of Molecular Pathology, Graduate School of Medicine, University of Tokyo, 7-3-1 Hongo, Bunkyo-ku, Tokyo 113-0033, Japan. Phone: 81-3-5841-3345; Fax: 81-3-5841-3354; E-mail: miyazono-ind@umin.ac.jp.

doi:10.1158/0008-5472.CAN-07-1522

also promotes cell survival under certain conditions (8). TGF-β has been shown to promote cell survival through activation of the phosphatidylinositol 3-kinase (PI3K)-Akt signaling pathway, which plays a key role in mediating cell survival downstream of tyrosine kinase signaling, including that mediated by insulin-like growth factor or platelet-derived growth factor (PDGF).

Several studies have revealed recently that targeting of TGF-β signaling in breast cancer cells by various strategies, such as use of soluble TβR-II antagonist, neutralizing TGF-β antibody, or small-molecule type I receptor kinase inhibitors, can prevent cancer metastasis (10–13). Consistent with this, we showed previously that systemic gene transfer of Smad7 inhibits the metastasis of mouse mammary carcinoma JygMC(A) cells in an *in vivo* experimental model (14). Thus, TGF-β is considered one of the molecular targets in the treatment of breast cancer metastasis. However, little is known about the downstream signaling pathways of TGF-β involved in the process of metastasis of breast cancer.

Here, we present the first evidence that the roles played by TGF-β signaling in survival of breast cancer cells are mediated by induction of differentially expressed in chondrocytes 1 (DEC1, also known as SHARP2 and Stra13). DEC1 is a basic helix-loop-helix transcription factor, which is frequently overexpressed in certain cancers, including breast carcinomas (15). Correlation between the expression of DEC1 and tumor grade in breast cancer has been reported (16). We found that TGF-β induces DEC1 and prevents apoptosis of mouse mammary carcinoma cells. In addition, we show that a dominant-negative mutant of DEC1 (dnDEC1) prevents lung and liver metastasis of breast cancer cells *in vivo*. Our observations thus provide new insight into the molecular mechanisms governing TGF-β–mediated survival of tumors and may aid the development of new strategies for cancer therapy.

Materials and Methods

Cell culture and reagents. Mouse mammary carcinoma 4T1 cells and mouse mammary epithelial NMuMG cells were obtained from American Type Culture Collection. 4T1 cells were cultured in DMEM containing 10% fetal bovine serum (FBS), 100 units/mL penicillin, and 100 μg/mL streptomycin. NMuMG cells were maintained in DMEM containing 10% FBS, 10 μg/mL insulin, and antibiotics. Mouse mammary carcinoma JygMC(A) cells were cultured as described previously (14). Cells were grown in a 5% CO_2 atmosphere at 37°C. The TβR-I kinase inhibitor used in the present study, A-44-03, is a dihydrochloride salt form of A-77-01 (17). SB431542 was obtained from Sigma. LY294002 and STI571 (imatinib mesylate/Gleevec) were purchased from Calbiochem and Novartis Pharma, respectively. The contents of one capsule of STI571 were dissolved in 17 mL of distilled water, centrifuged, filtered, and used as 10 mmol/L stock solution (18).

Apoptosis assays. For detection of cytosolic DNA ladder formation, both floating cells and adherent cells were collected and lysed with a lysis buffer [20 mmol/L Tris-HCl (pH 7.5), 10 mmol/L EDTA, 0.5% Triton X-100]. Cell extracts were incubated with 0.1 mg/mL RNase A and 0.2 mg/mL proteinase K at 42°C for 1 h. DNA was purified by standard phenol-chloroform extraction and ethanol precipitation. Dry DNA pellets were then resuspended in TE containing 0.2 mg/mL RNase A, and samples were electrophoretically separated on 2% agarose gel containing 0.01% ethidium bromide. For terminal deoxynucleotidyl transferase–mediated dUTP nick end labeling (TUNEL) assays, cells were fixed in 4% paraformaldehyde. After permeabilization in PBS containing 0.1% Triton X-100 and 0.1% sodium citrate, reagents of the *In situ* Cell Death Detection kit (TMR red, Roche Diagnostics) were added. The nuclei were stained by 4′,6-diamidino-2-phenylindole (DAPI). Fluorescence was examined using an IX71 microscope (Olympus) and measured by the Integrated Intensity Program of MetaVue (Molecular Devices Corp.).

Quantitative real-time reverse transcription-PCR. Total RNAs were extracted using Trizol reagent (Invitrogen). First-strand cDNAs were synthesized using the SuperScript First-Strand Synthesis System (Invitrogen) with oligo(dT) primers. Quantitative real-time reverse transcription-PCR (RT-PCR) was done as described previously (13). The primer sequences were as follows: mouse DEC1: 5′-GAAGCACGTGAAAGCATTGACA (forward) and 5′-CCCGACAAATCACCAGCTTG (reverse); mouse plasminogen activator inhibitor-1 (PAI-1): 5′-CCACAAAGGTCTCATGGACCAT (forward) and 5′-TGAAAGTGTTGTGCCCTCCAC (reverse); and mouse hypoxanthine phosphoribosyltransferase 1 (HPRT1): 5′-CTGGTTAAGCAGTACAGCCCCA (forward) and 5′-GGTCCTTTTCACCAGCAAGCT (reverse). All samples were run in duplicate in each experiment. Values were normalized to mouse HPRT1.

Immunoblotting. Cells were lysed after various treatments with NP40 lysis buffer [20 mmol/L Tris-HCl (pH 7.5), 150 mmol/L NaCl, 1% NP40, 1% aprotinin, 1 mmol/L phenylmethylsulfonyl fluoride]. The supernatants were measured for protein concentrations, and those with equal amounts of total proteins were applied to 8.5% SDS-gel electrophoresis, followed by semidry transfer of the proteins to Pall FluoroTrans W membrane (Pall Life Sciences). Nonspecific binding of proteins to the membrane was blocked by incubation in TBS-T buffer [50 mmol/L Tris-HCl (pH 7.4), 150 mmol/L NaCl, 0.1% Tween 20] containing 5% skim milk. Separated proteins were immunoblotted with anti-Flag antibody (M2; Sigma), anti–phospho-Smad2 ($Ser^{465/467}$) antibody (Cell Signaling Technology), or anti-Smad2/3 antibody (BD Transduction Laboratories). Detection of immunoblotted proteins was done by enhanced chemiluminescence.

Construction of recombinant adenoviruses and adenoviral infection. Recombinant E1-deleted adenoviral vectors carrying cDNAs encoding β-galactosidase (*LacZ*) reporter gene, Smad6, Smad7, and c-Ski were described previously (19). cDNAs encoding Flag-tagged dominant-negative TβR-II (dnTβR-II), which lacks the intracellular domain of TβR-II, and Flag-tagged human DEC1 were subcloned into the pAxCAwtit cassette cosmid (Takara). Each cosmid carrying the expression unit and adenovirus DNA terminal protein complex was cotransfected into E1 transcomplemental cell line 293 cells. The recombinant adenoviruses generated by homologous recombination were isolated. For adenoviral infection, 5×10^5 of JygMC(A) cells per well in six-well plates were infected with adenovirus vectors at 30 to 300 plaque-forming units per cell.

Microarray analysis. mRNAs were extracted from JygMC(A) cells treated without or with TGF-β3 and those infected with Ad-*LacZ* or Ad-Smad7. Total RNAs were used to prepare cDNA and conduct oligonucleotide microarray analysis using GeneChip Mouse Genome 430 2.0 Array (Affymetrix) according to the manufacturer's instructions. FileMaker Pro software (Filemaker, Inc.) was used for statistical analysis.

RNA interference and oligonucleotides. Stealth small interfering RNA (siRNA) duplex oligoribonucleotides against mouse DEC1 were synthesized by Invitrogen. JygMC(A) cells were transfected in the presence of 150 pmol of either siRNA or control siRNA in a 500 μL volume with 7.5 μL LipofectAMINE RNAiMAX reagent (Invitrogen) per well of a six-well plate according to the manufacturer's protocols. To confirm knockdown of DEC1, cells were harvested 24 h after siRNA transfection and subjected to quantitative real-time RT-PCR.

Generation of JygMC(A) cells stably expressing dnDEC1. To establish JygMC(A) cells that stably express the dnDEC1 (Jyg-dnDEC1), a human DEC1 mutant lacking the basic region was cloned into pCAG-IRES-Puro expression vector (14). The pCAG-Flag-dnDEC1-IRES-Puro plasmid was introduced into JygMC(A) cells using LipofectAMINE 2000 reagent (Invitrogen). Stable clones were obtained by puromycin (Sigma) selection (8 μg/mL) in the culture medium, and several clones were then isolated by limiting dilution. JygMC(A) cells stably expressing the empty vector pCAG-empty-IRES-Puro (Jyg-empty) were used as a control.

***In vivo* experiment using JygMC(A) cells stably expressing dnDEC1.** To investigate *in vivo* tumor growth and metastasis of parental JygMC(A), Jyg-empty, or Jyg-dnDEC1, a mouse experimental model of metastasis was used. All animal procedures were done in the animal experiment laboratory of the Japanese Foundation for Cancer Research (JFCR) according to the guidelines proposed by the Science Council of Japan. Female BALB/c *nu/nu*

mice (4 weeks of age) were purchased from Charles River Japan. Mice were maintained under specific pathogen-free conditions. Parental JygMC(A), Jyg-empty, or Jyg-dnDEC1 cells (10^7 cells) were xenografted into the mammary fat pad of each mouse ($n > 6$ mice per group). Primary tumor growth and metastases were examined as described previously (14). Statistical differences to controls were validated by the two-sided Student's t test. $P < 0.05$ was considered significant.

Results

Antiapoptotic effects of exogenous and endogenous TGF-β on murine normal epithelial and breast cancer cells. Murine breast carcinoma JygMC(A) cells undergo cell death when cultured in low concentrations of serum. Interestingly, TGF-β promoted the survival of the JygMC(A) cells under these conditions, and the low-molecular-weight TβR-I kinase inhibitor A-44-03 further enhanced the death of JygMC(A) cells (Fig. 1*A*). Regulation of cell survival by TGF-β signaling was further investigated by DNA ladder formation and TUNEL assay. DNA ladder formation was observed under serum-free conditions, but not in the presence of 10% serum (Fig. 1*B*). TGF-β suppressed DNA ladder formation, whereas A-44-03 enhanced it under these conditions, indicating that inhibition of TGF-β signaling leads to cell death by apoptosis in JygMC(A) cells. Apoptosis of JygMC(A) cells was also observed in a TUNEL assay under serum-free conditions, and the cell survival–promoting effect of TGF-β was confirmed (Fig. 1*C* and *D*). Another low-molecular-weight TβR-I kinase inhibitor SB431542, which is less potent than A-44-03 (17), also induced apoptosis of JygMC(A) cells, although 10 μmol/L SB431542 was required to induce their apoptosis in the presence of 1 ng/mL TGF-β3 (Supplementary Fig. S1*A* and *B*). These findings suggest that exogenous TGF-β promotes the survival of JygMC(A) cells and that endogenous TGF-β produced by JygMC(A) cells functions as a prosurvival factor for these cells.

To determine whether the survival-promoting effect of TGF-β is limited to JygMC(A) cells, we examined TGF-β–mediated survival of other mammary epithelial cells (i.e., murine breast cancer 4T1 cells and murine normal epithelial NMuMG cells). Similar to JygMC(A) cells, A-44-03 induced apoptosis of 4T1 cells (Fig. 2*A* and *B*). Although A-44-03 failed to significantly induce apoptosis of NMuMG cells, TGF-β potently enhanced their survival. It is important to note that Smad2 was significantly phosphorylated in the absence of exogenous TGF-β in JygMC(A) cells and 4T1 cells, but only very weakly in NMuMG cells (Fig. 2*C*, compare *lane 2* and *lane 5* with *lane 8*). These findings suggest that cell survival mediated by autocrine TGF-β signaling may be related to tumor growth and metastasis.

Roles of PDGF receptor and Akt signaling in the promotion of cell survival by TGF-β. To elucidate the mechanisms by which TGF-β promotes the survival of JygMC(A) cells, we did cDNA microarray analysis. Smad7 inhibits TGF-β family signaling through direct binding to activated type I receptors as well as by other mechanisms (20). The *Smad7* gene was infected into JygMC(A) cells by an adenoviral vector, and genes regulated by TGF-β signals were determined with the Affymetrix GeneChip Mouse Genome 430 2.0 Array (Supplementary Table S1). The results of the microarray analysis were confirmed by quantitative real-time RT-PCR analysis. Among 59 genes regulated by TGF-β, we were interested in the *Pdgfb* gene (encoding PDGF-B chain) because it has been reported to mediate TGF-β–induced proliferation of glioma cells, and epigenetic regulation of the human *PDGFB* gene is closely related to the prognosis of glioblastoma (21). We confirmed by real-time RT-PCR that expression of PDGF-B mRNA

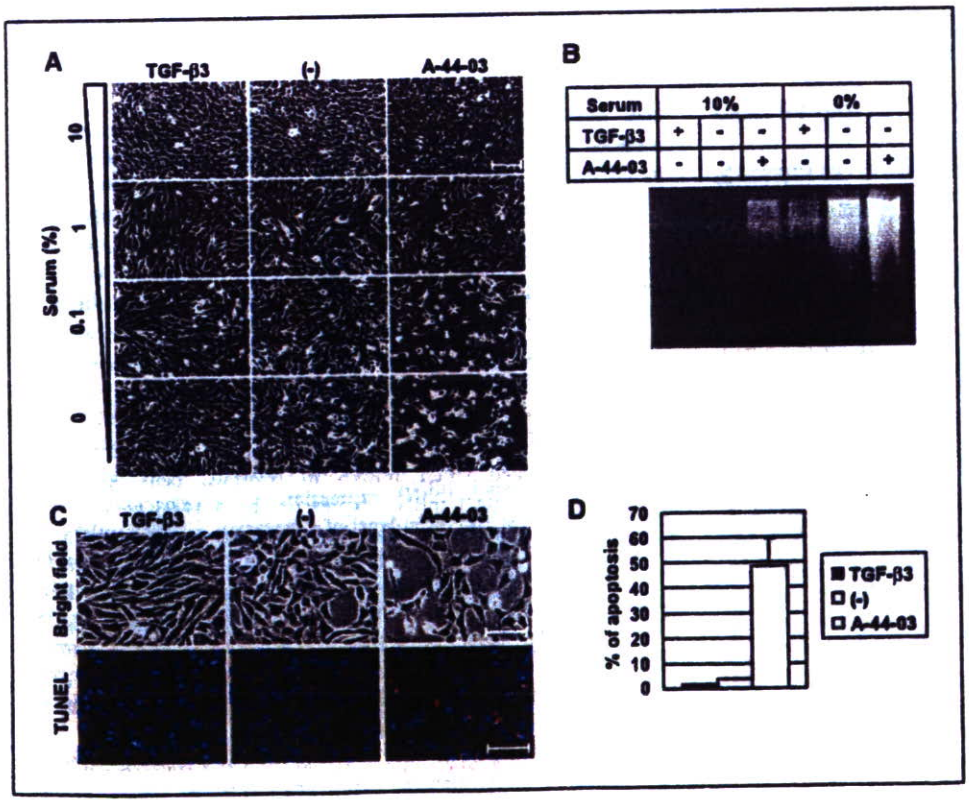

Figure 1. Antiapoptotic effects of TGF-β on JygMC(A) cells. *A*, JygMC(A) cells were treated with TGF-β3 (1 ng/mL) or A-44-03 (1 μmol/L) in the presence of various concentrations of FBS (between 0% and 10%) for 48 h. Cells were observed under phase-contrast microscopy. *Bar*, 100 μm. *B*, JygMC(A) cells were treated with TGF-β3 (1 ng/mL) or A-44-03 (1 μmol/L) in the presence or absence of FBS for 48 h. Apoptotic cell death was assessed by DNA fragmentation assay. Characteristic DNA ladders were observed after ethidium bromide staining. *C*, JygMC(A) cells were treated with TGF-β3 (1 ng/mL) or A-44-03 (1 μmol/L) in the presence of FBS for 48 h. Cells were fixed and observed under phase-contrast microscopy (*top*) or subjected to TUNEL staining (*bottom*). Cell nuclei were counterstained with DAPI. *Red*, TUNEL; *blue*, DAPI. *Bar*, 100 μm. *D*, the percentage of TUNEL-positive cells among DAPI-positive cells in *C* was determined. *Columns*, mean of triplicate determinations; *bars*, SD.

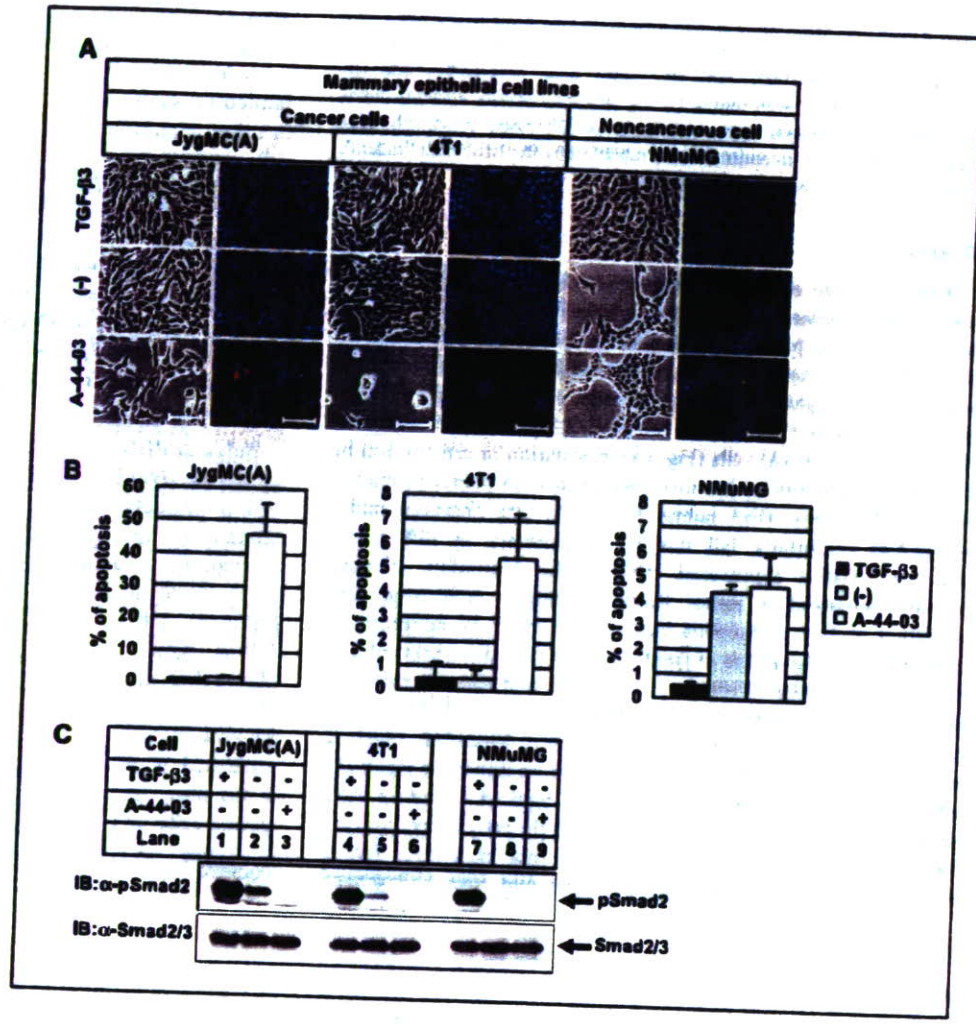

Figure 2. TGF-β–mediated survival of mouse mammary epithelial cells. *A*, mammary cancer cells [JygMC(A) cells and 4T1 cells] and normal mammary epithelial cells (NMuMG cells) were treated with TGF-β3 (1 ng/mL) or A-44-03 (1 μmol/L) in the absence of FBS for 48 h. Cells were observed under phase-contrast microscopy (*left*) and subjected to TUNEL staining (*right*). *Red*, TUNEL; *blue*, DAPI. *Bar*, 100 μm. *B*, the percentage of TUNEL-positive cells among DAPI-positive cells was determined. *Columns*, mean of triplicate determinations; *bars*, SD. *C*, mammary cancer cells [JygMC(A) cells and 4T1 cells] and normal mammary epithelial cells (NMuMG cells) were treated with TGF-β3 (1 ng/mL) or A-44-03 (1 μmol/L) in the absence of FBS for 1 h. Cell lysates were subjected to immunoblotting (*IB*) with anti–phospho-Smad2 (*pSmad2*) antibody (*top*) and anti-Smad2/3 antibody (*bottom*).

was induced by TGF-β and suppressed by A-44-03 (Supplementary Fig. S2*A*).

Because it has been reported that TGF-β induces cell survival by activation of PI3K-Akt signaling (8), we examined whether an inhibitor of PDGF receptor signaling (STI571) or one of Akt signaling (LY294002) inhibits the promotion of cell survival by TGF-β under serum-free conditions. Although STI571 and LY294002 induced apoptosis of JygMC(A) cells in the absence of TGF-β, neither of them was able to induce apoptosis of JygMC(A) cells in the presence of exogenous TGF-β (Supplementary Fig. S2*B* and *C*). Although the combination of STI571 and LY294002 strongly induced apoptosis of JygMC(A) cells in the absence of TGF-β, it induced their apoptosis only weakly in the presence of TGF-β (Supplementary Fig. S2*B* and *C*).

Promotion of the survival of JygMC(A) cells by TGF-β is mediated by DEC1. Because PDGF receptor and PI3K-Akt signaling may not be the major signaling pathways involved in TGF-β–mediated cell survival of JygMC(A) cells, we further analyzed the genes regulated by TGF-β in JygMC(A) cells. Among the 59 genes regulated by TGF-β, we found that mRNA for *Dec1* (also termed *basic helix-loop-helix domain containing, class B2*) was strongly suppressed by Smad7 in the presence of serum (Supplementary Table S1). We confirmed the effects of TGF-β and A-44-03 on the transcription of DEC1 mRNA in the presence or absence of 10% serum (Fig. 3*A*). Quantitative real-time RT-PCR analysis revealed that A-44-03 suppressed the transcription of DEC1 mRNA in JygMC(A) cells in the presence and absence of 10% serum. Although TGF-β induced the transcription of DEC1 mRNA only weakly in the presence of 10% serum, significant increase in DEC1 mRNA by TGF-β was detected in the absence of serum in JygMC(A) cells. SB431542 also suppressed the expression of DEC1 mRNA in serum-free conditions (Supplementary Fig. S1*C*). We also assessed the expression of DEC1 in serum-free conditions using other mammary epithelial cells (Fig. 3*A*). Similar to JygMC(A) cells, 4T1 cells exhibited modest induction of DEC1 mRNA by TGF-β and strong suppression of expression of it by A-44-03. Although TGF-β strongly induced DEC1 mRNA in NMuMG cells, significant suppression of DEC1 mRNA expression by A-44-03 could not be observed because the basal level of expression of DEC1 mRNA in NMuMG cells was very low. It should be noted that these profiles of expression of DEC1 mRNA correlated closely with the pattern of apoptosis induced by A-44-03 treatment, as shown in Fig. 2*B*. TGF-β has also been shown to promote cell survival in human breast cancer MDA-MB-231 cells (22). In agreement with this finding, induction of DEC1 mRNA by TGF-β was also observed in MDA-MB-231 cells (Supplementary Fig. S3).

We next examined the effect of DEC1 on the apoptosis induced by A-44-03 by infection of adenovirus carrying DEC1 cDNA.

Expression of DEC1 protein after adenovirus infection was confirmed by immunoblot analysis (Fig. 3*B*). A-44-03 induced apoptosis of JygMC(A) cells in the absence of serum, and neither control adenovirus carrying the *LacZ* gene nor stimulation by TGF-β significantly affected the apoptosis induced by A-44-03 (Fig. 3*C* and *D*). However, infection of adenovirus carrying DEC1 resulted in potent suppression of apoptosis of the cells induced by A-44-03. These findings suggested that the promotion of the survival of JygMC(A) cells by TGF-β is mediated by DEC1.

Promotion of survival of JygMC(A) cells by TGF-β is mediated in Smad-dependent fashion. To determine whether TGF-β prevents apoptosis of JygMC(A) cells in Smad-dependent fashion and whether the expression of DEC1 is indeed mediated by the TGF-β signaling pathway, we examined the effects of adenoviruses carrying various negative regulators of TGF-β signaling on TGF-β–mediated cell survival. Among the negative regulators of TGF-β signaling, c-Ski binds to Smad complexes and suppresses their transcriptional activity as a transcriptional corepressor, whereas dnTβR-II binds to TGF-β but fails to transduce intracellular signals and acts as a dominant-negative inhibitor of Smad-dependent and non-Smad pathways (20, 23). Smad7 inhibits both TGF-β and BMP signaling, whereas Smad6 inhibits BMP but not TGF-β signaling efficiently (20). As shown in Fig. 4*A*, infection of these adenoviruses resulted in efficient expression of transfected proteins in JygMC(A) cells. Analysis of the expression of a TGF-β target gene, *PAI-1*, revealed that dnTβR-II, Smad7, and c-Ski effectively suppressed TGF-β signaling, whereas Smad6 failed to do so (Fig. 4*B*). Apoptosis of JygMC(A) cells was determined by TUNEL assay in the absence or presence of TGF-β under serum-free conditions (Fig. 4*C*). dnTβR-II, Smad7, and c-Ski, but not Smad6, induced apoptosis of JygMC(A) cells in the presence and absence of TGF-β. Because c-Ski inhibits TGF-β signaling through interaction with Smad2/3 and Smad4, these findings suggest that TGF-β induces survival of JygMC(A) cells in Smad-dependent fashion. We also confirmed that expression of DEC1 is suppressed by dnTβR-II as well as by Smad7 and c-Ski (Fig. 4*D*), indicating that the expression of DEC1 is mediated by TGF-β signaling.

Silencing endogenous DEC1 abolishes the prosurvival effect of TGF-β. Because forced expression of DEC1 rescued the induction of apoptosis of JygMC(A) cells by A-44-03, we further examined the role of endogenous DEC1 in TGF-β–promoted survival of JygMC(A) cells by the siRNA method. As shown in Fig. 5*A*, we efficiently knocked down endogenous DEC1 mRNA in the cells by transfection of siRNA targeting DEC1. Interestingly, reduction of DEC1 mRNA expression resulted in significant increase in the number of apoptotic cells in the absence or presence of TGF-β under serum-free conditions (Fig. 5*B* and *C*). These findings suggest that the promotion of cell survival by TGF-β is dependent on DEC1, which is transcriptionally induced by endogenous TGF-β.

dnDEC1 induces apoptosis of JygMC(A) cells and inhibits their metastasis. Acquisition of resistance to apoptosis is thought to be related to the metastatic phenotype of cancer cells (1). Because DEC1 seemed to act as an important regulator of survival of breast cancer cells, we examined whether the DEC1-mediated survival signal is involved in the process of metastasis. We used a mutant of DEC1 lacking the basic region (dnDEC1), which acts in dominant-negative fashion (24). JygMC(A) cells, which stably express dnDEC1, were established and two stable clones, termed Jyg-dnDEC1#1 and Jyg-dnDEC1#2, were used for further investigations (Fig. 6*A*, *top*). As expected, both Jyg-dnDEC1#1 cells and

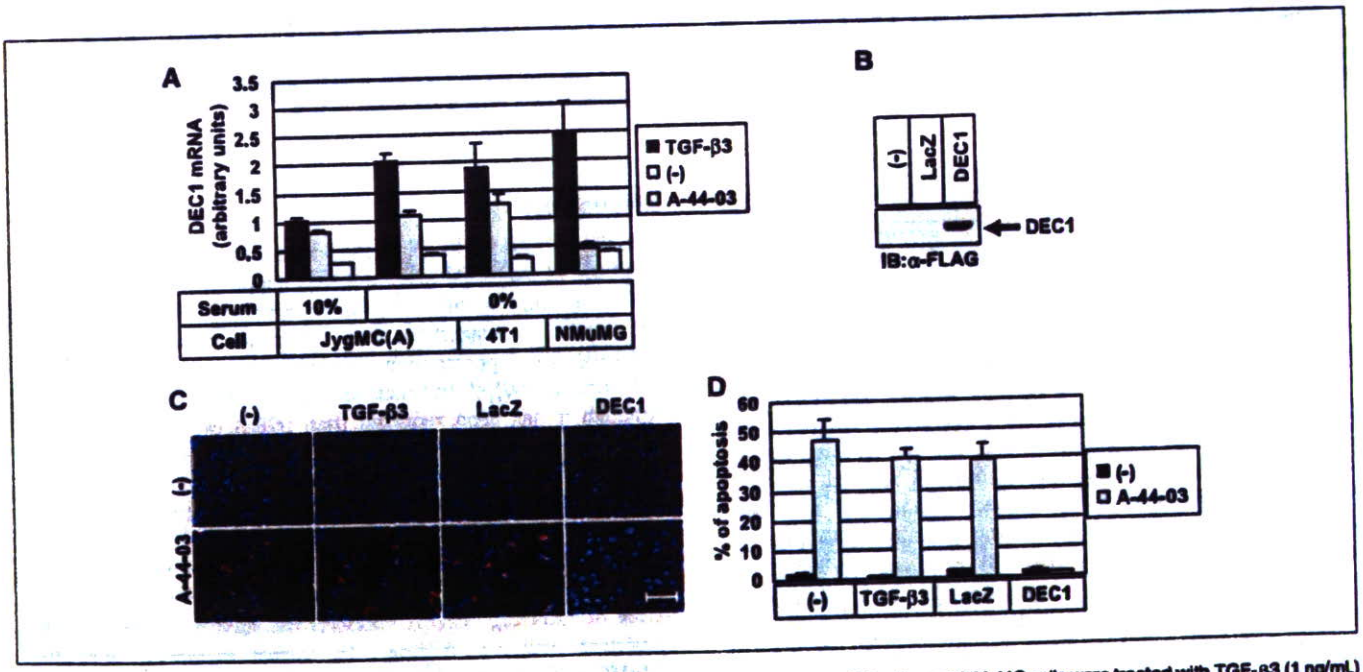

Figure 3. Promotion of survival of JygMC(A) cells by TGF-β is mediated by DEC1. *A*, JygMC(A) cells, 4T1 cells, and NMuMG cells were treated with TGF-β3 (1 ng/mL) or A-44-03 (1 μmol/L) in the presence of the indicated concentrations of FBS for 24 h. Expression of DEC1 mRNA was examined by quantitative real-time RT-PCR. Each value has been normalized to the expression of HPRT1. *Columns*, mean of duplicate determinations; *bars*, SD. *B*, JygMC(A) cells were infected with adenoviruses carrying full-length *LacZ* or DEC1, and expression of DEC1 protein was determined by immunoblotting analysis of the cell lysates 24 h after infection. *C*, JygMC(A) cells were infected with each adenovirus 12 h before A-44-03 treatment and incubated for 48 h with A-44-03 (1 μmol/L). Cells were subjected to TUNEL staining. *Red*, TUNEL; *blue*, DAPI. *Bar*, 100 μm. *D*, the percentage of TUNEL-positive cells among DAPI-positive cells was determined. *Columns*, mean of triplicate determinations; *bars*, SD.

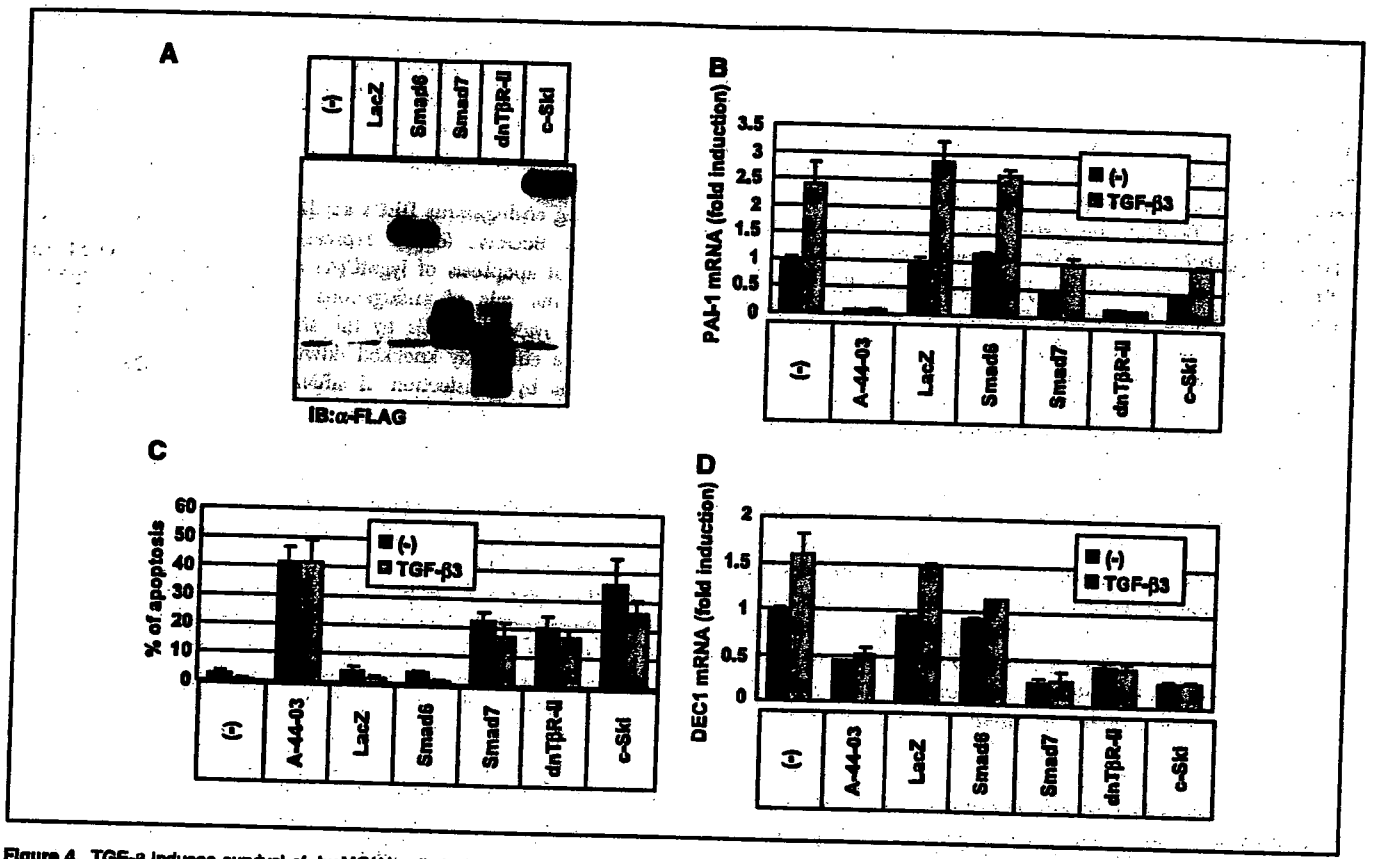

Figure 4. TGF-β induces survival of JygMC(A) cells in Smad-dependent fashion. *A*, JygMC(A) cells were infected with adenoviruses carrying full-length *LacZ*, Smad6, Smad7, dnTβR-II, and c-Ski cDNAs. Expression of recombinant protein was determined by immunoblotting analysis of each cell lysate. *B*, suppression of target genes for TGF-β was measured by quantitative real-time RT-PCR. JygMC(A) cells were infected with each adenovirus 12 h before treatment with or without TGF-β3 (1 ng/mL for 24 h). Total RNAs were extracted, and the levels of expression of *PAI-1* gene were examined by quantitative real-time RT-PCR. Fold changes relative to the uninfected control without TGF-β3 treatment are indicated. Each value has been normalized to the expression of HPRT1. *Columns*, mean of duplicate determinations; *bars*, SD. *C*, the percentage of TUNEL-positive cells among DAPI-positive cells was determined. Twelve hours after adenoviral infection, the cells were treated with or without TGF-β3 (1 ng/mL) under serum-free conditions for 48 h and subjected to TUNEL staining. *Columns*, mean of triplicate determinations; *bars*, SD. *D*, expression of DEC1 mRNA in JygMC(A) cells infected with the adenoviruses described in *B* was examined by quantitative real-time RT-PCR. Fold changes relative to the uninfected control without TGF-β3 treatment are indicated. Each value is presented as in *B*.

Jyg-dnDEC1#2 cells underwent apoptotic cell death in serum-starved conditions (Fig. 6*A*, *bottom*). Furthermore, overexpression of the dnDEC1 mutant induced apoptosis even in the presence of TGF-β, suggesting that dnDEC1 effectively antagonizes TGF-β–mediated cell survival.

Finally, we investigated the growth and metastatic potential of Jyg-dnDEC1 cells in *in vivo* experiments. After s.c. inoculation into nude mice and formation of primary tumors, JygMC(A) cells metastasize to lung and liver within 3 weeks (14). Growth of the primary tumors and metastases to lung and liver in mice bearing parental JygMC(A), Jyg-empty, and Jyg-dnDEC1 cells are shown in Fig. 6*B* to *D*. Growth of the primary tumors did not differ significantly between the mice bearing parental JygMC(A), Jyg-empty, and Jyg-dnDEC1 cells (Fig. 6*B*). However, the lungs and livers in the mice bearing Jyg-dnDEC1#1 or Jyg-dnDEC1#2 weighed less than those in mice bearing parental JygMC(A) or Jyg-empty (Fig. 6*D*, *top*). Intriguingly, stable expression of dnDEC1 in JygMC(A) cells produced few metastatic nodules in the lungs and liver (Fig. 6*C* and *D*, *bottom*). These findings indicate that DEC1 contributes to the metastasis of JygMC(A) cells by promoting cell survival without affecting primary tumor growth *in vivo*.

Discussion

In the present study, we showed that serum starvation induced apoptosis of JygMC(A) cells and that suppression of endogenous TGF-β signaling by the TβR-I kinase inhibitors strongly enhanced this apoptosis, suggesting that autocrine TGF-β signaling in JygMC(A) cells supports their own survival.

Autocrine TGF-β induces survival of breast cancer cells. Although it has been reported that TGF-β causes apoptosis in certain types of cells (8), apoptosis is induced by exogenous TGF-β at much higher concentrations than those required for inhibition of cell growth. Lei et al. (22) reported that disruption of autocrine TGF-β signaling by the ectopic expression of a soluble TGF-β type III receptor induces apoptosis of human breast cancer MDA-MB-231 cells. Their findings indicate that TGF-β, acting in autocrine fashion, supports the survival of cancer cells, consistent with our findings. In normal mammary epithelial NMuMG cells, which exhibited low basal TGF-β signaling activity, a cell survival–promoting effect of TGF-β was observed with the addition of exogenous TGF-β, whereas A-44-03 failed to significantly enhance apoptosis (see Fig. 2*A–C*). By contrast, in breast cancer JygMC(A) cells and 4T1 cells, phosphorylation of Smad2 was observed even in the absence of TGF-β stimulation (see

Fig. 2C), and A-44-03 potently induced apoptosis of these cells. We measured the amounts of TGF-βs but could not detect active forms of TGF-βs in the conditioned medium of these cells.[6] Apparently, latent TGF-β is activated on the surface of cells and immediately binds to the receptors, preventing the detection of active TGF-β in the conditioned medium. Thus, during the progression of cancer, cancer cells might gain the ability to activate TGF-β signaling in autocrine fashion, and this property might protect them from various apoptotic stimuli, enabling their survival.

TGF-β has been reported to act as a prosurvival factor via Akt/protein kinase B signaling (22, 25, 26). Moreover, TGF-β has been reported to induce the expression of PDGF in certain types of cells, which may lead to activation of PI3K-Akt signaling. We reported previously that TGF-β enhances the growth of MG63 osteosarcoma cells through induction of PDGF-A and that this growth-stimulatory activity of TGF-β is abolished by treatment with STI571/Gleevec (18). In addition, TGF-β was shown to stimulate the proliferation of glioblastoma cells via induction of PDGF-B, which may be related to the poor prognosis of human glioma (21). However, in the present study, we showed that pharmacologic inhibition of PDGF receptor signaling by STI571 or that of PI3K-Akt signal by LY294002 failed to induce apoptosis of JygMC(A) cells in the presence of exogenous TGF-β and that the combination of ST1571 and LY294002 only partially antagonized TGF-β–induced cell survival. These findings suggest that survival signals other than PI3K-Akt must be present in these cells.

TGF-β induces survival of breast cancer cells through DEC1. We further analyzed DNA microarray data to identify the downstream molecule(s) involved in TGF-β–mediated cell survival and found that TGF-β induces the expression of DEC1, which may antagonize serum deprivation–induced apoptosis. DEC1, also known as SHARP2 and Stra13, is widely expressed in most normal tissues (27, 28) and associated with developmental events in many cells and regulation of circadian rhythms (29–31). DEC1 has been suggested to serve as a downstream target of TGF-β (32). Separate from TGF-β signaling, DEC1 is also induced in response to hypoxia (33). DEC1 is overexpressed in various cancers, including breast cancer, colorectal cancer, pancreatic cancer, non–small cell lung cancer, and oligodendroglioma (15, 34–37). Moreover, a significant correlation between DEC1 expression and grade in breast carcinomas has been reported (16). Although DEC1 has been reported to antagonize serum deprivation–induced apoptosis of colon carcinoma (38), the role of DEC1 in TGF-β–induced cell survival has not been elucidated. In the present study, we found that levels of expression of DEC1 in the breast cancer JygMC(A) cells and 4T1 cells were much higher than that in the normal mammary epithelial NMuMG cells and that DEC1 plays a critical role in TGF-β–mediated survival of breast carcinoma cells, strongly suggesting that expression of DEC1 is important for cancer progression.

DEC1 was originally identified as a basic helix-loop-helix transcription factor (39). DEC1 binds to CACGTG E-boxes (24, 32) and represses the transcription of many target genes (30, 40, 41). In the present study, we showed that dnDEC1, which competes with endogenous DEC1 for DNA binding, induces apoptosis of JygMC(A) cells and prevents metastasis, suggesting that TGF-β–induced DEC1 prevents apoptosis of JygMC(A) cells at the transcriptional level. Li et al. (42) reported that the antiapoptotic protein survivin is a target of DEC1 and suggested that survivin is responsible for the survival of cells induced by DEC1. However, our microarray analysis data indicated that survivin is not induced by TGF-β in JygMC(A) cells, and we were unable to identify other well-known apoptosis-related genes. Identification of the transcriptional target(s) of DEC1 responsible for the survival of breast cancer cells is thus required in the future.

DEC1 is involved in the metastasis of breast cancer induced by TGF-β signaling. We have reported previously that systemic gene transfer of Smad7 inhibits the metastasis of JygMC(A) cells through induction of EMT and suppression of cell migration (14). In the present study, we showed that suppression of the DEC1-mediated survival signal caused apoptosis, whereas forced

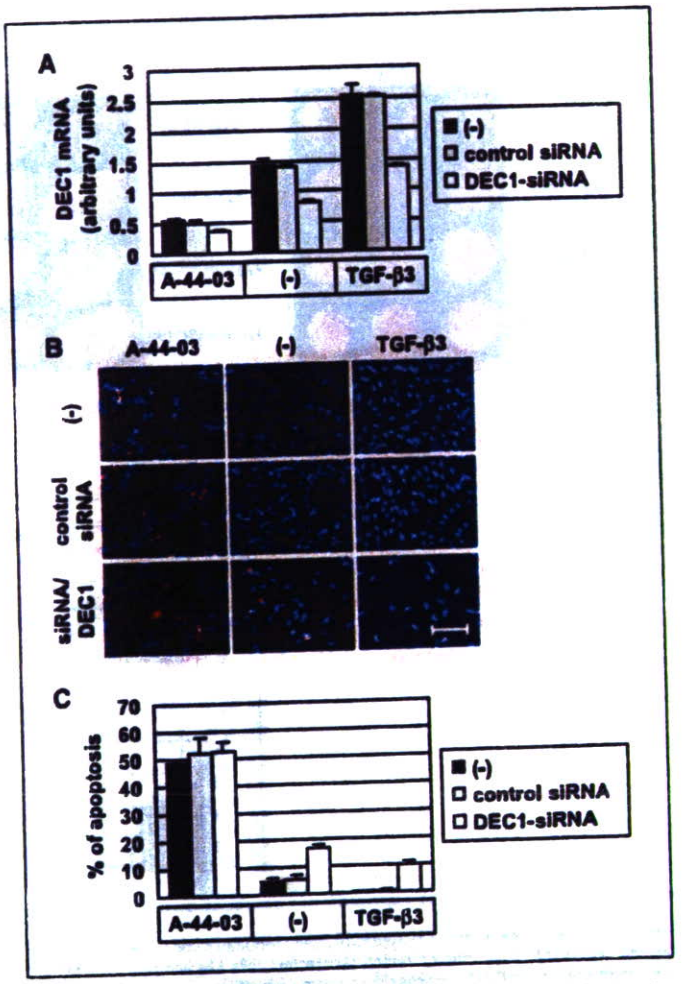

Figure 5. Silencing of endogenous DEC1 abolishes TGF-β–induced survival of JygMC(A) cells. *A*, JygMC(A) cells were transfected with control siRNA or DEC1-targeting siRNA, and levels of expression of DEC1 mRNAs were determined by quantitative real-time RT-PCR analysis. Each value has been normalized to the expression of HPRT1. *Columns*, mean of duplicate determinations; *bars*, SD. *B*, 12 h after transfection, cells were cultured in serum-free medium with TGF-β3 (1 ng/mL) or A-44-03 (1 μmol/L) for 48 h. Cells were subjected to TUNEL staining. *Red*, TUNEL; *blue*, DAPI. *Bar*, 100 μm. *C*, the percentage of TUNEL-positive cells among DAPI-positive cells was determined. *Columns*, mean of triplicate determinations; *bars*, SD.

[6] S. Ehata, unpublished data.

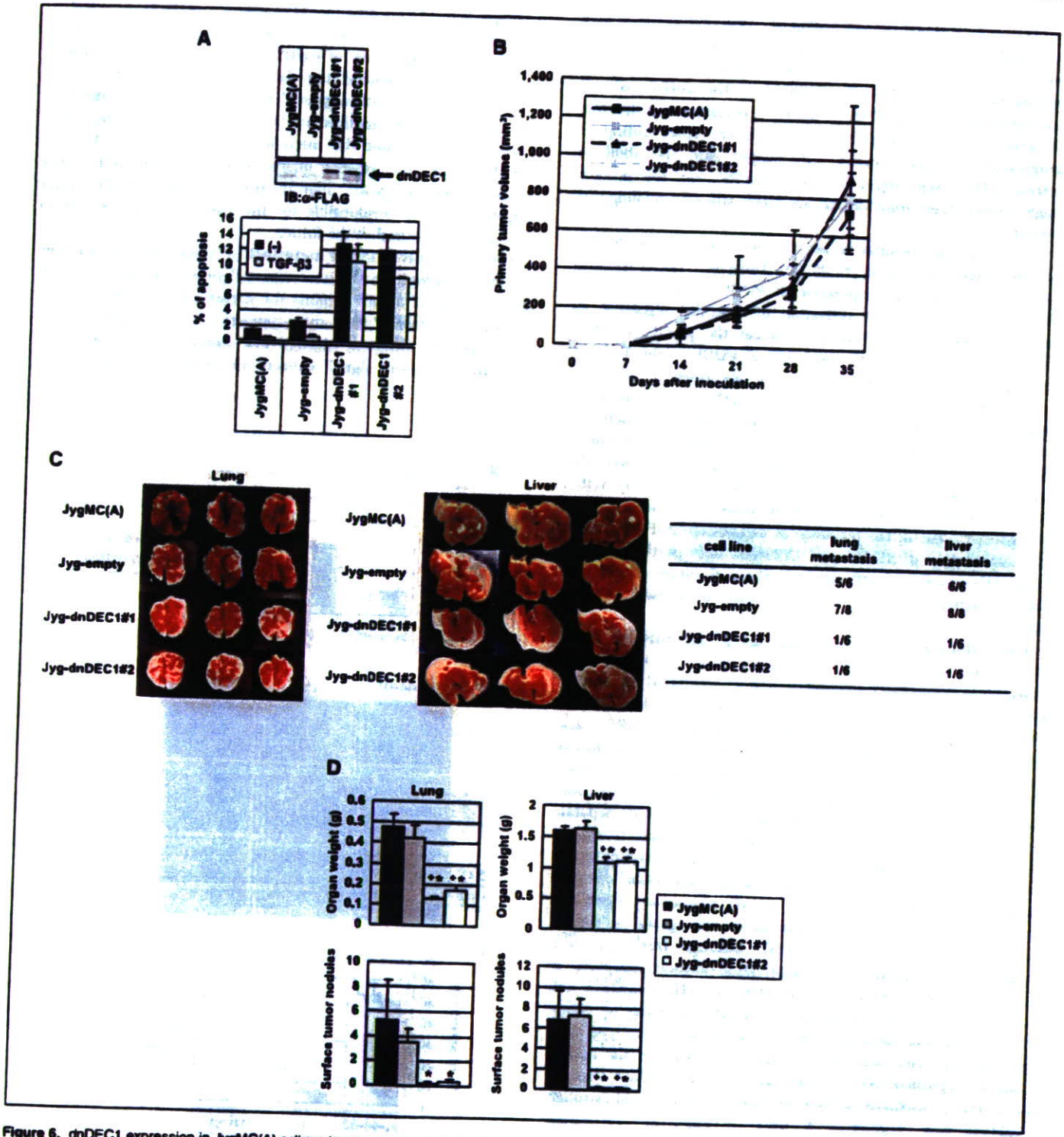

cell line	lung metastasis	liver metastasis
JygMC(A)	5/6	6/6
Jyg-empty	7/8	8/8
Jyg-dnDEC1#1	1/6	1/6
Jyg-dnDEC1#2	1/6	1/6

Figure 6. dnDEC1 expression in JygMC(A) cells reduces tumor metastasis of xenografted mice. *A*, establishment of JygMC(A) cells that stably express the dnDEC1. Parental JygMC(A) cells, empty vector-transfected cells (Jyg-empty), and two stable clones of dnDEC1-expressing cells (Jyg-dnDEC1#1 and Jyg-dnDEC1#2) were examined for dnDEC1 expression by immunoblotting using anti-Flag antibody (*top*). Equal amounts of parental JygMC(A) cells, Jyg-empty cells, Jyg-dnDEC1#1, and Jyg-dnDEC1#2 were cultured in serum-free medium with TGF-β3 (1 ng/mL) for 48 h and subjected to TUNEL staining (*bottom*). The percentage of TUNEL-positive cells among DAPI-positive cells was determined. *Columns*, mean of triplicate determinations; *bars*, SD. *B* to *D*, JygMC(A), Jyg-empty, Jyg-dnDEC1#1, or Jyg-dnDEC1#2 cells were injected into the mammary fat pad of BALB/c *nu/nu* mice. All mice were euthanized on day 35 post-transplantation or earlier if they seemed moribund. *B*, the effects of dnDEC1 expression in JygMC(A) cells on primary tumor growth. The longest axis (*a*) and shortest perpendicular axis (*b*) of the primary tumor were measured every 7 d, and tumor volume was calculated using the formula 0.4 ab^2. *Points*, mean; *bars*, SD. *C*, the effects of dnDEC1 expression in JygMC(A) cells on liver and lung metastasis. Representative photographs showing lungs with mediastinum (*top left*) and livers (*top right*) from mice subjected to injection with the indicated cells. Incidences of metastasis in lung and liver are shown as macroscopic metastases/total mice (*bottom*). *D*, quantitative analysis of the weights of tumor-bearing lung and liver (*top*) and the number of visually observable surface tumor nodules in lung and liver (*bottom*). These experiments were repeated twice with similar results. *Columns*, mean of all sacrificed mice; *bars*, SE. +, $P < 0.05$, statistically significant difference compared with JygMC(A); *, $P < 0.05$, statistically significant difference compared with Jyg-empty.